

**Land surface modeling informed by earth observation data  
toward understanding blue–green–white water fluxes in High Mountain Asia**

Buri, Pascal; Fatichi, Simone; Shaw, Thomas E.; Fyffe, Catriona L.; Miles, Evan S.; McCarthy, Michael J.; Kneib, Marin; Ren, Shaoting; Menenti, Massimo; More Authors

**DOI**

[10.1080/10095020.2024.2330546](https://doi.org/10.1080/10095020.2024.2330546)

**Publication date**

2024

**Document Version**

Final published version

**Published in**

Geo-Spatial Information Science

**Citation (APA)**

Buri, P., Fatichi, S., Shaw, T. E., Fyffe, C. L., Miles, E. S., McCarthy, M. J., Kneib, M., Ren, S., Menenti, M., & More Authors (2024). Land surface modeling informed by earth observation data: toward understanding blue–green–white water fluxes in High Mountain Asia. *Geo-Spatial Information Science*, 27(3), 703–727. <https://doi.org/10.1080/10095020.2024.2330546>

**Important note**

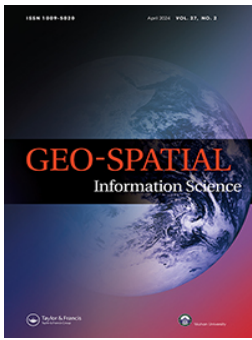
To cite this publication, please use the final published version (if applicable).  
Please check the document version above.

**Copyright**

Other than for strictly personal use, it is not permitted to download, forward or distribute the text or part of it, without the consent of the author(s) and/or copyright holder(s), unless the work is under an open content license such as Creative Commons.

**Takedown policy**

Please contact us and provide details if you believe this document breaches copyrights.  
We will remove access to the work immediately and investigate your claim.



## Land surface modeling informed by earth observation data: toward understanding blue–green–white water fluxes in High Mountain Asia

Pascal Buri, Simone Fatichi, Thomas E. Shaw, Catriona L. Fyffe, Evan S. Miles, Michael J. McCarthy, Marin Kneib, Shaoting Ren, Achille Jouberton, Stefan Fugger, Li Jia, Jing Zhang, Cong Shen, Chaolei Zheng, Massimo Menenti & Francesca Pellicciotti

**To cite this article:** Pascal Buri, Simone Fatichi, Thomas E. Shaw, Catriona L. Fyffe, Evan S. Miles, Michael J. McCarthy, Marin Kneib, Shaoting Ren, Achille Jouberton, Stefan Fugger, Li Jia, Jing Zhang, Cong Shen, Chaolei Zheng, Massimo Menenti & Francesca Pellicciotti (22 Mar 2024): Land surface modeling informed by earth observation data: toward understanding blue–green–white water fluxes in High Mountain Asia, *Geo-spatial Information Science*, DOI: [10.1080/10095020.2024.2330546](https://doi.org/10.1080/10095020.2024.2330546)

**To link to this article:** <https://doi.org/10.1080/10095020.2024.2330546>



© 2024 Wuhan University. Published by Informa UK Limited, trading as Taylor & Francis Group.



[View supplementary material](#)



Published online: 22 Mar 2024.



[Submit your article to this journal](#)



Article views: 437



[View related articles](#)



[View Crossmark data](#)

# Land surface modeling informed by earth observation data: toward understanding blue–green–white water fluxes in High Mountain Asia

Pascal Buri<sup>a</sup>, Simone Fatichi<sup>b</sup>, Thomas E. Shaw<sup>a,c</sup>, Catriona L. Fyffe<sup>c</sup>, Evan S. Miles<sup>a</sup>, Michael J. McCarthy<sup>a</sup>, Marin Kneib<sup>d,e</sup>, Shaoting Ren<sup>f</sup>, Achille Jouberton<sup>a,g</sup>, Stefan Fugger<sup>a,g</sup>, Li Jia<sup>h</sup>, Jing Zhang<sup>i</sup>, Cong Shen<sup>h</sup>, Chaolei Zheng<sup>h</sup>, Massimo Menenti<sup>h,j</sup> and Francesca Pellicciotti<sup>a,c</sup>

<sup>a</sup>Swiss Federal Institute for Forest, Snow and Landscape Research WSL, Birmensdorf, Switzerland; <sup>b</sup>Department of Civil and Environmental Engineering, National University of Singapore, Singapore, Singapore; <sup>c</sup>Institute of Science and Technology Austria (ISTA), Klosterneuburg, Austria; <sup>d</sup>Institute of Environmental Geosciences, Université Grenoble Alpes, Grenoble, France; <sup>e</sup>Department of Atmospheric and Cryospheric Sciences, University of Innsbruck, Innsbruck, Austria; <sup>f</sup>State Key Laboratory of Tibetan Plateau Earth System, Environment and Resources (TPESER), Institute of Tibetan Plateau Research, Chinese Academy of Sciences, Beijing, China; <sup>g</sup>Institute of Environmental Engineering, ETH Zurich, Zurich, Switzerland; <sup>h</sup>State Key Laboratory of Remote Sensing Science, Aerospace Information Research Institute, Chinese Academy of Sciences, Beijing, China; <sup>i</sup>National Space Sciences Center, Chinese Academy of Sciences, Beijing, China; <sup>j</sup>Faculty of Civil Engineering and Geosciences, Delft University of Technology, Delft, The Netherlands

## ABSTRACT

Mountains are important suppliers of freshwater to downstream areas, affecting large populations in particular in High Mountain Asia (HMA). Yet, the propagation of water from HMA headwaters to downstream areas is not fully understood, as interactions in the mountain water cycle between the cryo-, hydro- and biosphere remain elusive. We review the definition of blue and green water fluxes as liquid water that contributes to runoff at the outlet of the selected domain (*blue*) and water lost to the atmosphere through vapor fluxes, that is evaporation from water, ground, and interception plus transpiration (*green*) and propose to add the term *white water* to account for the (often neglected) evaporation and sublimation from snow and ice. We provide an assessment of models that can simulate the cryo-hydro-biosphere continuum and the interactions between spheres in high mountain catchments, going beyond disciplinary separations. Land surface models are uniquely able to account for such complexity, since they solve the coupled fluxes of water, energy, and carbon between the land surface and atmosphere. Due to the mechanistic nature of such models, specific variables can be compared systematically to independent remote sensing observations – providing vital insights into model accuracy and enabling the understanding of the complex watersheds of HMA. We discuss recent developments in spaceborne earth observation products that have the potential to support catchment modeling in high mountain regions. We then present a pilot study application of the mechanistic land surface model Tethys & Chloris to a glacierized watershed in the Nepalese Himalayas and discuss the use of high-resolution earth observation data to constrain the meteorological forcing uncertainty and validate model results. We use these insights to highlight the remaining challenges and future opportunities that remote sensing data presents for land surface modeling in HMA.

## ARTICLE HISTORY

Received 6 July 2023  
Accepted 8 March 2024

## KEYWORDS

Land surface modeling; remote sensing; High Mountain Asia (HMA); blue-green water; cryosphere-hydrosphere-biosphere continuum; snow; glaciers; high mountain water cycle

## 1. Introduction


Mountains act as water towers of the world, supplying crucial freshwater to adjacent downstream areas (Bandhopyadhyay et al. 1997; Immerzeel et al. 2020; Viviroli et al. 2007). Changes in the mountain water cycle have immediate implications for runoff production, ecosystem functioning, and water resources (Cauvy-Fraunié and Dangles 2019; Milner et al. 2017; Stibal et al. 2020), affecting large populations particularly in High Mountain Asia (HMA; Immerzeel, Van Beek, and Bierkens 2010; Nie et al. 2021; Pritchard 2019; Yao et al. 2022). Yet, the propagation of water from HMA headwaters to downstream areas is not fully understood, as the

mountain water cycle is shaped by complex interactions between the hydrosphere and biosphere which are rarely studied or modeled together.

Here, we provide a perspective on recent efforts to model the high mountain water cycle in an integrated manner, considering the cryosphere-hydrosphere-biosphere continuum. We review and update the definition of blue and green water fluxes, and consider the models that can represent that continuum and the interactions between spheres going beyond disciplinary separations. Traditionally, glaciers are modeled with glacier models, snow processes with snow models, hydrology by conceptual simplified models, and vegetation is either ignored or considered as a separate

**CONTACT** Pascal Buri  pascal.buri@wsl.ch

This article has been corrected with minor changes. These changes do not impact the academic content of the article.

 Supplemental data for this article can be accessed online at <https://doi.org/10.1080/10095020.2024.2330546>

© 2024 Wuhan University. Published by Informa UK Limited, trading as Taylor & Francis Group.

This is an Open Access article distributed under the terms of the Creative Commons Attribution License (<http://creativecommons.org/licenses/by/4.0/>), which permits unrestricted use, distribution, and reproduction in any medium, provided the original work is properly cited. The terms on which this article has been published allow the posting of the Accepted Manuscript in a repository by the author(s) or with their consent.

field of research. When these distinct processes and compartments are taken together, this is mostly in simplified, conceptual, or empirical glacio-hydrological models. We argue that we can advance beyond this separation, which is still dominant in classical hydrology, between streamflow generation processes, whether from rain, snow, glaciers, or groundwater, and water stored or transformed by the biosphere, such as evapotranspiration. This move can be enabled by land surface models, which are established for large-scale simulations, but have rarely been used for distributed catchment simulations and even less so for the high mountain water cycle. Here, we show an example of how land surface models, in combination with a new generation of spaceborne remote-sensing data, offer powerful tools to shed light on processes until now ignored or that have remained unquantified.

## 2. A new perspective for modeling high mountain catchments

### 2.1. Blue-green-white water fluxes

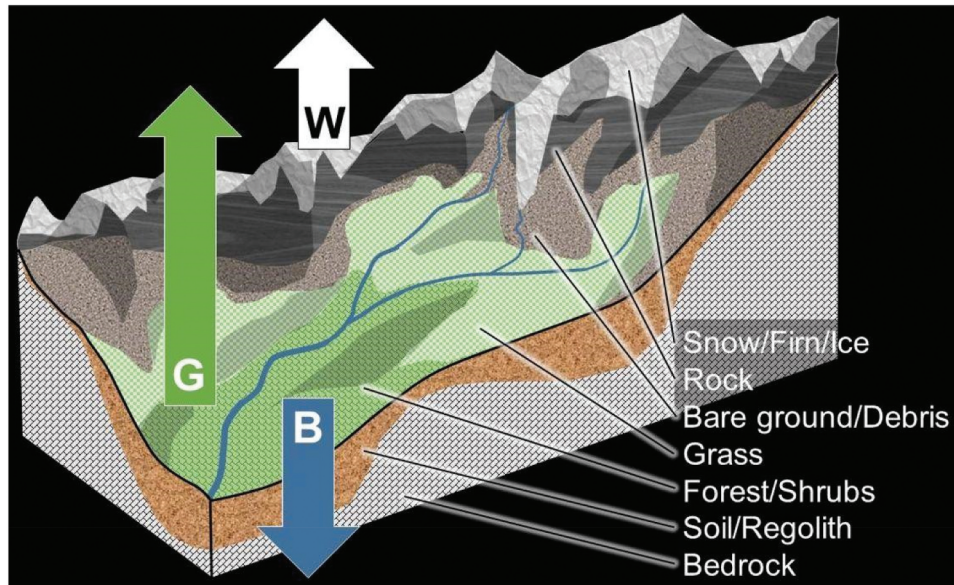
Understanding the partition between blue-green water fluxes is crucial for quantifying the hydrology of mountain areas. Blue-green water fluxes have been often defined in the context of water management and agricultural research (Falkenmark 1995; Falkenmark and Rockström 2006; Feng, Yang, and Han 2021; Rockström et al. 2009) to quantify water resources readily available for use (blue water) versus vapor flows that go back to the atmosphere (green water) (Sood, Prathapar, and Smakhtin 2014). A more holistic definition, however, is missing. Here, we use a definition based on a catchment water balance (Figure 1(a)), where blue and green water fluxes are calculated for given spatial and temporal scales. Blue-green water must be defined as fluxes, because the fate of water in a given storage is a priori generally unknown for a spatial domain (e.g. a catchment) and for a temporal period (e.g. annually). Given these assumptions, blue water encompasses liquid/flowing water that contributes to runoff at the outlet of the selected domain and is thus accessible for (human) use, whereas green water comprises water lost to the atmosphere through vapor fluxes, that is evaporation from water, ground, and interception plus transpiration. We propose here to call moisture fluxes due to evaporation and sublimation from snow and ice, which are often unaccounted for in hydrological models, as *white water*. Note that as stated above, water storage within the domain, which can be of many types, does not fall into either category until it contributes to runoff or vapor fluxes. Practically, the blue water flux flowing out of a defined domain determines the freshwater supply to downstream regions, while

green water fluxes are key to transfer precipitated water back into the atmosphere, with the potential to move it across zones and regions (De Kok et al. 2018; Keune and Miralles 2019; Rockström et al. 2023). Storage in the cryosphere (e.g. snow, ice, permafrost), biosphere (e.g. plant water content) and pedosphere (e.g. soil moisture, groundwater) can potentially become blue, green or white water, according to energy fluxes, topography, and catchment characteristics, even though for certain storage types (such as groundwater or plant water content), the fate can be largely predicted a priori.

A few examples illustrate these potential transformations: i) water stored in the soil can become blue water if e.g. washed out by additional rain, or it can become green water if evaporated at the soil surface or through plant transpiration; ii) solid precipitation or an existing snowpack can become blue water if melted and transferred into a river that leaves the domain, white water if sublimated or green water if melted and subsequently evaporated by the soil or vegetation; iii) liquid precipitation will become blue water as soon as it contributes to discharge as infiltration excess runoff, but can remain stored in the soil or wetlands.

In high mountainous areas, the complex terrain, with high spatial heterogeneity of land surface conditions and rapid changes in elevation and microclimate, affects the water cycle in many ways. The cryosphere-hydrosphere-biosphere responses and feedbacks (e.g. melting snow feeding vegetation, snowpack persistence preventing the beginning of the growing season) are often complex and nonlinear, which hinders a proper quantification of different water budget components in traditional large-scale climate change impact assessments (Fan et al. 2019). For example, glaciers and snow can act as key water reservoirs during droughts in HMA (Pritchard 2019) but anthropogenic warming is anticipated to increase atmospheric evaporative demands (Vicente-Serrano et al. 2014), with the consequence of potentially shifting the partition of the catchment water balance by turning blue into green water (Falkenmark and Rockström 2006; Jolly et al. 2005; Mastrotheodoros et al. 2020; Orth and Destouni 2018). The role of air temperature in accelerating ice and snow melt has been at the center of scientific attention (e.g. Huss and Hock 2018; Kraaijenbrink et al. 2017). However, its role in changing the ablation partition from sublimation-dominated to melt-dominated (Fyffe et al. 2021), in enhancing evapotranspiration (ET) and diminishing blue water fluxes due to increased productivity at short-time scales (Mastrotheodoros et al. 2020) or vegetation succession at longer terms (Carnahan, Amundson, and Hood 2019) has been studied much less. Understanding how vegetation processes affect the availability of blue water from HMA catchments with glaciers, snow, and liquid precipitation varying

## a) Blue, green and white water fluxes at catchment scale



## b) Importance of off-glacier land cover in a glacierized catchment

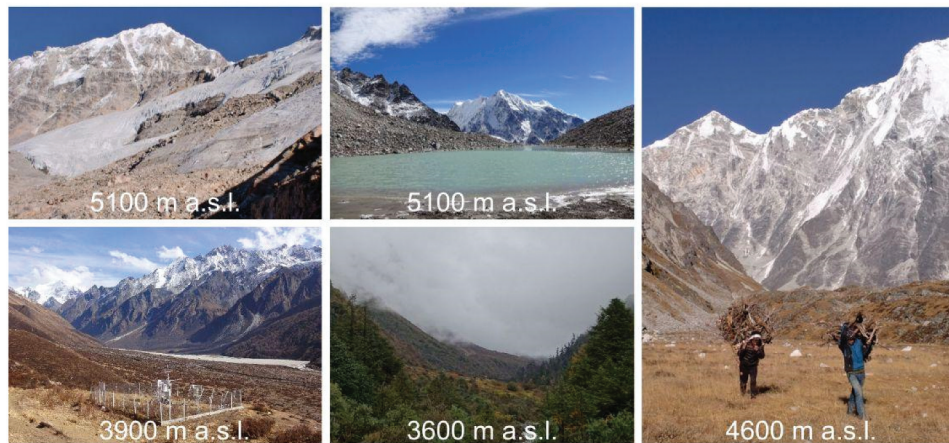


**Figure 1.** (a) Conceptual representation of a mountain watershed with typical land cover and updated blue-green-white water fluxes scheme: blue water (B; liquid/flowing water contributing to runoff), green water (G; water lost to the atmosphere through evapotranspiration), and white water (W; evaporation and sublimation from snow and ice); (b) Landscapes at different altitudes in the upper Langtang Valley (Nepal), the catchment in our pilot study (photos: P. Buri).

sub-seasonally and with elevation, is a pressing but challenging research question. The science community is, however, at a stage where models of increasing sophistication, and abilities can i) resolve all processes leading to blue, green, and white water fluxes' formation simultaneously and in a unified framework (rather than through distinct analyses) and ii) tackle their complex transformation in a warming climate. This step is strongly supported by the increasing diversity, accuracy, and resolution of remote sensing products

## 2.2. Land surface modelling in High Mountain Asia

The tools that can account for the complexity of processes generating blue-green-white water fluxes are

*land surface models*, i.e. numerical models that solve the coupled fluxes of water, energy, and carbon between the land surface and atmosphere (Blyth et al. 2021; R. A. Fisher and Koven 2020). Land surface models simulate biophysical processes in (most of) the critical zone – Earth's dynamic skin, e.g. from the top of the vegetation canopy through the soil and potentially down to fresh bedrock and the bottom of the groundwater in multiple grid cells (Grant and Dietrich 2017). To date, most land surface models focus on global or regional scales with horizontal grid dimensions of  $0.25\text{--}1^\circ$  (equivalent to about 25–100 km at mid-latitudes), and are thus not able to resolve energy and water fluxes at sufficient spatial detail to capture local heterogeneities and the complexity of high elevation topography. Most importantly, microclimatic and topographic effects leading to complex energy inputs

and lateral flows of water in the surface and subsurface are often not solved, with few exceptions (Bierkens et al. 2015; Fan et al. 2019; Ivanov, Bras, and Vivoni 2008; Mastrotheodoros et al. 2020; Wood et al. 2011). This is particularly relevant in mountainous domains such as glacierized watersheds in HMA. Many of the land surface models available today were developed several decades ago, and only recently included detailed mechanistic representations of the entire soil – plant – atmosphere continuum (Bonan et al. 2021; Kennedy et al. 2019). They still struggle in representing vegetation dynamics (Fisher and Koven 2020), or specific processes such as the role of soil structure (Fatichi et al. 2020) and thus might oversimplify the link between soil moisture and transpiration (Clark et al. 2011; De Kauwe et al. 2015; Sheffield, Wood, and Roderick 2012; Teuling 2018). Mountain glaciers, and especially those with a debris-covered surface, which are common in HMA (estimated at 8–12% of glacierized area; Herreid and Pellicciotti 2020; Kraaijenbrink et al. 2017; Scherler, Wulf, and Gorelick 2018), have been completely neglected in current land surface-modeling applications.

Another category of models commonly used to understand water resources in glacierized catchments are glacio-hydrological models. Numerous studies have applied distributed conceptual glacio-hydrological models in HMA, i.e. models that use parameterization and conceptual description of hydrological processes and in particular calculate snow and glacier melt based on (calibrated) degree-day melt factors (see a non-exhaustive list of the most advanced model approaches in Table 1). Temperature index models (also called degree-day models) are based on an assumed relationship between ablation and air temperature usually expressed in the form of positive temperature sums (Hock 2003). These models often simplify the components of the hydrological cycle, and mostly ignore vegetation processes. Due to the general scarcity of in-situ data at high elevations, these models, requiring little input data and relatively low computation time, represent a reasonable way to estimate glacier- and snow melt for multiyear or decadal time scales, from the catchment (Ragetti, Immerzeel, and Pellicciotti 2016) to regional (Kraaijenbrink et al. 2021; Kraaijenbrink et al. 2017) and global scales (Rounce et al. 2023). However, they depend on parameters calibrated for site-specific and present-day conditions, limiting their transferability in space (Gabbi et al. 2014) and time (Fatichi et al. 2016; Marzeion et al. 2020), and for extreme conditions. This makes simulations from such models less robust, especially in a regionally variable, non-stationary climate. Importantly, while focusing on the cryosphere, glacio-hydrological models neglect green fluxes, either entirely, or by oversimplifying these processes (e.g. vegetation dynamics, soil–vegetation interactions)

through empirical equations (e.g. Priestley – Taylor eq. in Ragetti et al. 2015; Hamon eq. in Sorg et al. 2014) or considering the total ET amount as a residual of the water balance. Glacierized catchments, even located at very high altitudes as in HMA, are not solely covered by glaciers – a substantial part consists of rock, soils, and vegetation, and, in some cases, dense forest (e.g. in the Langtang Valley shown in Figure 1(b)). The treeline in HMA is among the highest in the world (Miehe et al. 2007), and vegetation (mostly shrub) has been observed to develop even on the debris-covered tongues of Himalayan glaciers (Racoviteanu, Nicholson, and Glasser 2021). Plant transpiration might thus represent a major part of the water budget (Fatichi and Pappas 2017; Yang et al. 2023), even in high mountain areas with scarce vegetation (Buri et al. 2023). The large variability in microclimatic effects, soil-moisture availability, and stomata sensitivity to water stress (Lansu et al. 2020; Lin et al. 2015; Mastrotheodoros et al. 2019; Teuling et al. 2010) hinder a quantification based on simple parameterizations.

To our knowledge, only one land surface modeling study has been conducted in HMA to date: it resolved the full surface energy and mass balance for the Langtang catchment in Nepal, accounting mechanistically for the relevant processes of the cryo-, hydro- and biosphere (e.g. clean ice, snow and sub-debris melt, soil and vegetation dynamics, and lateral flow routing; Buri et al. 2023). We use this in this study to show the potential and challenges of modeling high mountain blue-green-white water fluxes and their dynamics. This represents a research frontier and demands innovative use of multiple datasets for model confirmation.

### 2.3. Use of earth observation data for land surface modelling

There is a dramatic lack of high-elevation in-situ data in HMA (Cogley 2011; Pellicciotti et al. 2012; Pritchard 2021; Winiger, Gumpert, and Yamout 2005), which results in a general difficulty of capturing land–atmosphere interactions with field measurements (Hiller, Zeeman, and Eugster 2008). Remotely sensed observations at high resolution offer a great opportunity to develop and evaluate land surface models while reducing uncertainties in model initialization and simulation (Zhao and Li 2015). Remote sensing has permitted an unrivaled understanding of key changes in the cryosphere (Dehecq et al. 2019; Hugonnet et al. 2021; Miles et al. 2021) and biosphere (e.g. Maina et al. 2022; Zhu et al. 2016) of HMA over the past decades. The systematic combination of remote sensing and catchment models has proven vital for the understanding of the complex catchments of HMA (e.g. Ragetti, Immerzeel, and Pellicciotti 2016). Model structure and complexity, however,

**Table 1.** Examples of high-resolution glacio-hydrological studies with fully distributed, temperature index models focusing on glacierized mountain catchments in High Mountain Asia (non-exhaustive list).

Catchment (Region)	Area (elevation range)	Target model period	Model	Resolution (space and time)	Reference	URL
Zhadang (W-Nyainqentanglha, China)	8 km <sup>2</sup> (5560–6080 m a.s.l.)	2011–2014	DHSVM-GDM	20 m; hourly	Zhang et al. (2016)	<a href="https://doi.org/10.1002/2016JD025434">https://doi.org/10.1002/2016JD025434</a>
Pheriche (E-Himalayas, Nepal)	146 km <sup>2</sup> (4260–8850 m a.s.l.)	2012–2015	DHSVM-GDM	100 m; hourly	Mimeau et al. (2019)	<a href="https://doi.org/10.5194/hess-23-3969-2019">https://doi.org/10.5194/hess-23-3969-2019</a>
Pailung (SE-Nyainqentanglha, China)	24 km <sup>2</sup> (4650–5960 m a.s.l.)	1975–2018	TOPKAPI-ETH	30 m, hourly	Jouberton et al. (2022)	<a href="https://doi.org/10.1073/pnas.2109796119">https://doi.org/10.1073/pnas.2109796119</a>
Langtang (Central Himalayas, Nepal)	360 km <sup>2</sup> (3800–7234 m a.s.l.)	1987–1997	Based on TAC <sup>D</sup>	200m, daily	Konz et al. (2007)	<a href="https://doi.org/10.5194/hess-11-1323-2007">https://doi.org/10.5194/hess-11-1323-2007</a>
Langtang & Balforo (Central Himalayas, Nepal; Karakoram, Pakistan)	360 km <sup>2</sup> (3800–7234 m a.s.l.) and 1415 km <sup>2</sup> (3173–8611 m a.s.l.)	1957 – 2100	A glacio-hydrological model	90 m, daily	Immerzeel et al. (2013)	<a href="https://doi.org/10.1038/ngeo1896">https://doi.org/10.1038/ngeo1896</a>
Langtang (Central Himalayas, Nepal)	585 km <sup>2</sup> (1406–7234 m a.s.l.)	2003–2010	TOPKAPI-ETH	100m, daily	Immerzeel et al. (2014)	<a href="https://doi.org/10.1002/2013WR014506">https://doi.org/10.1002/2013WR014506</a>
Langtang (Central Himalayas, Nepal)	350 km <sup>2</sup> (3650–7225 m a.s.l.)	2012–2013	TOPKAPI-ETH	100 m, hourly	Ragetti et al. (2015)	<a href="https://doi.org/10.1016/j.advwatres.2015.01.013">https://doi.org/10.1016/j.advwatres.2015.01.013</a>
Chon Kemin (W-Tien Shan, Kyrgyzstan)	1,037 km <sup>2</sup> (1500–4760 m a.s.l.)	1955–2099	GERM	200 m, daily	Sorg et al. (2014)	<a href="https://doi.org/10.1088/1748-9326/9/10/104018">https://doi.org/10.1088/1748-9326/9/10/104018</a>
Hunza River Basin (Karakoram, Pakistan)	14,234 km <sup>2</sup> (1494–7788 m a.s.l.)	2001–2003	TOPKAPI-ETH	500 m, daily	Pellicciotti et al. (2012)	<a href="https://doi.org/10.1659/MRD-JOURNAL-D-11-00092.1">https://doi.org/10.1659/MRD-JOURNAL-D-11-00092.1</a>
Hunza River Basin (Karakoram, Pakistan)	13,715 km <sup>2</sup> (1494–7788 m a.s.l.)	2000–2050	TOPKAPI-ETH	500 m, daily	Ragetti et al. (2013)	<a href="https://doi.org/10.1002/wrcr.20450">https://doi.org/10.1002/wrcr.20450</a>

needs to lend itself to a combination with spatial data from remote sensing, requiring a distributed approach and a physical representation of processes.

Remote sensing data from different platforms have become increasingly available (Small 2021), and we present here a selection of them (Section 3) that shows how these new remotely sensed data sets can be exploited to advance our understanding of blue-green-white water interactions in high elevation catchments when combined with land surface models. We show a possible way forward in the land surface modeling of HMA by presenting a pilot study to inform, constrain, and evaluate simulations from a detailed mechanistic model with the help of high resolution remote sensing data (Section 4).

### 3. Advances in remote sensing of the cryo-, bio- and hydrosphere in High Mountain Asia

In this section, we provide a selection of current earth observation products, albeit without any claim to be exhaustive, that have the potential to be integrated into land surface modeling to resolve blue-green-white water fluxes, specifically in HMA.

#### 3.1. Cryosphere

##### 3.1.1. Glacier thinning and mass change

The glacier mass balance gives an integrated assessment of the model's ability to represent both precipitation and melt processes in a distributed way. The elevation change of a glacier surface can be measured from space using radar or laser altimetry, gravimetry, or by differencing digital elevation models derived from synthetic aperture radar or stereo optical imagery (Berthier et al. 2023). These methods have been increasingly applied at local, regional, and global scales (Hugonnet et al. 2021; Jakob and Gourmelen 2023; Shen, Jia, and Ren 2022; Wang, Yi, and Sun 2021). At local scales, longer-term glacier elevation change measurements are possible due to declassified spy satellite data (e.g. Bhattacharya et al. 2021; Dehecq et al. 2020), which can prove very useful for assessing long-term glacier mass balance changes (e.g. Jouberton et al. 2022).

However, contemporary geodetic mass balance measurements only provide a single mass balance value per glacier. A substantial step forward compared to this approach is the derivation of distributed glacier mass balance estimates. These are derived by solving the continuity equation (Miles et al. 2021; Van Tricht et al. 2021), which requires distributed estimates of geodetic glacier thinning (e.g. Hugonnet et al. 2021), glacier surface motion (e.g. Gardner, Fahnestock, and Scambos 2022; Millan et al. 2023) and ice thickness (e.g. Farinotti et al. 2019), which are all directly or partly derived from remote sensing data.

##### 3.1.2. Snow cover

To reproduce the mountain water cycle accurately, land-surface models must accurately represent all the processes that cause snow to accumulate or lose mass. The assessment of distributed snow cover serves as a proxy for precipitation amounts and timing, precipitation phase partitioning and snow melt dynamics (e.g. Armstrong et al. 2019; Misra et al. 2020; Rittger, Painter, and Dozier 2013). Snow cover remote sensing primarily involves manually delineating snow-covered areas in optical satellite images, or generating Normalized Difference Snow Index (NDSI) images from green and near shortwave infrared spectral bands, and delineating snow-covered areas automatically via a thresholding approach (e.g. Hall, Riggs, and Salomonson 1995). Clouds must be identified and removed before the creation of binary or fractional snow cover maps. Fractional snow cover can then be calculated for a region by integrating snow coverage, while snowline elevation can be calculated, for example, through optimization approaches using an elevation model (e.g. Krajčí et al. 2014).

The most commonly used snow cover satellite products are Moderate Resolution Imaging Spectroradiometer (MODIS) Snow Cover (daily, 500 m; Hall and Riggs 2020), and the NDSI products from the Landsat and Sentinel satellites (16-day, <30 m). Planet, Digital Globe, and Pléiades all offer high-resolution optical imagery which can be used in a similar manner (Shaw et al. 2020a). As cloud computing has developed and access to such products has become easier, there has been a proliferation of snow cover studies at both regional and local scales (e.g. Zhang et al. 2021).

##### 3.1.3. Glacier albedo

By determining the net shortwave radiation absorbed at the glacier surface, glacier albedo is one of the key surface characteristics which controls the surface energy balance and can be used to indirectly assess if the snowfall and snow/ice melt distribution is correct. Glacier albedo can be estimated by satellite data (Naegeli et al. 2017; Naegeli, Huss, and Hoelzle 2019; Fugazza et al. 2019; Ren et al. 2021; Shaw et al. 2020b). So far, one glacier albedo product is widely used, which is MODIS (MOD10A1/MYD10A1 for snow albedo and MCD43A3 for land surface albedo). In addition, Landsat and Sentinel glacier albedos can also be obtained by a glacier albedo retrieval method using Google Earth Engine (Ren et al. 2021), and have been used in model calibration and validation (Buri et al. 2023).

##### 3.1.4. On-glacier debris cover

As supraglacial debris is an important component of many glaciers in HMA we also include information on generating debris-specific model inputs from remote-



sensing data. Modeling the glacio-hydrological response of debris-covered glaciers requires accounting for a number of additional glacier characteristics including debris thickness, as melt decreases exponentially as debris thickness increases (Fyffe et al. 2020; Östrem 1959). Supraglacial cliffs and ponds also enhance melt locally, partly compensating the debris influence (Buri et al. 2021; Miles et al. 2018). Debris extents have been derived at the global scale from optical images (Herreid and Pellicciotti 2020; Scherler, Wulf, and Gorelick 2018), and, recently, estimates of distributed debris thickness have been determined at regional and global scales (McCarthy et al. 2022; Rounce et al. 2021) using a combination of remotely sensed distributed surface mass balance products (Miles et al. 2021) and energy balance modeling. These products still have relatively high uncertainties, but other methods based on the inversion of remotely sensed debris surface temperature show good results at the local scale and could prove promising for catchment modeling (e.g. Foster et al. 2012; Kraaijenbrink et al. 2017; McCarthy 2018; Mihalcea et al. 2008; Rounce and McKinney 2014; Schauwecker et al. 2015). Depending on the method used and the scale at which debris thickness is derived, the influence of ice cliffs and ponds is somewhat implicitly already accounted for (McCarthy et al. 2022; Rounce et al. 2018). However, these contributions could be added explicitly, by combining ice cliff mapping from optical images (Miles et al. 2017; Watson et al. 2018; Kneib et al. 2021a, 2021b) with their enhancement factor relative to conventional sub-debris or clean ice melt (Miles et al. 2022).

## 3.2. Biosphere

### 3.2.1. Vegetation indices

An increasing number of data products have become available that map classical vegetation indices regionally and globally, leveraging surface reflectance observations, optical imagery, microwave, and laser ranging (e.g. Fang et al. 2019; Zeng et al. 2022). These products make it possible to characterize vegetation dynamics and structure at the global scale in a consistent way (e.g. Munier et al. 2018), with these indices being potentially directly comparable to land surface model outputs.

Both the *normalized difference vegetation index* (NDVI), which is a measure of vegetation greenness and density, and the *Enhanced Vegetation Index* (EVI) which allows corrections for atmospheric noise and canopy background signals (Huete et al. 2002) have been available globally since the 1980s from a combination of *Advanced Very High-Resolution Radiometer* (AVHRR; 1 km spatial resolution; daily temporal resolution) and *MODIS* data (500 m, daily). More recently NDVI is also available e.g. from Project

for *On-Board Autonomy-Vegetation* (PROBA-V; 2014 onwards; 300 m; 10 days) and *Sentinel-3* (2020 onwards; 300 m; 10 days).

*Leaf Area Index* (LAI) is defined as the total area of one-sided leaves over a unit of area on the ground (Chen and Black 1992). It quantifies the plants' capability to interact with the atmosphere as it determines the available area for the exchange of energy and mass between the canopy and the surrounding air (e.g. Law, Cescatti, and Baldocchi 2001). It can be mapped on a large scale using empirical or semi-empirical models that relate indices like NDVI or EVI to ground-observed LAI (Fang et al. 2019). Widely used global LAI products come from AVHRR (0.05° spatial resolution; daily temporal resolution), MODIS (500 m, 4 days), and more recently e.g. from PROBA-V (300 m, 10 days) and *Visible Infrared Imaging Radiometer Suite* (VIIRS; 300 m, 10 days).

A number of *gross primary productivity* (GPP) products have been made available combining various data sources and modeling techniques, including remotely sensed indices like NDVI and EVI, ground observations from flux towers, earth system model outputs, photosynthesis modeling, machine learning, and data assimilation. As an example, the MODIS GPP product (1 km spatial resolution, 8 day repeat cycle) uses MODIS derived NDVI together with meteorological observations as inputs for a light-use-efficiency model and is calibrated with global flux tower data (Running, Mu, and Zhao 2015). More recently, remotely sensed sun-induced fluorescence (SIF) retrievals were used as a proxy for GPP (e.g. Köhler et al. 2018; Maes et al. 2020; Pickering, Cescatti, and Duveiller 2022).

In theory, remotely sensed indices describing phenology and vegetation states have an enormous potential to aid the development, parameterization, and validation of mechanistic land surface models. However, the relatively coarse spatial resolution and often low overpass frequencies currently hinder robust applications in combination with land surface models, especially in HMA (with prevalent complex topography and frequent cloud cover).

### 3.2.2. Surface temperature

Surface temperature is a key variable with which to evaluate the performance of land-surface models because the major surface energy fluxes depend on it (e.g. longwave radiative, latent, and sensible heat, conductive heat flux). For this reason, comparing surface temperature simulated by a land-surface model with spaceborne surface temperature observations, i.e. thermal infrared radiation emitted by the land surface and atmospherically corrected, allows one to assess how well the model solves the surface energy balance, and therefore how well it represents the underlying physical processes. However, even though such a

comparison might appear straightforward, the capability of satellite sensors to observe only the uppermost layer of canopies or other surface properties, issues with emissivity specifications, and the fact that land-surface models might have quite distinct (and often integrated) methods of solving for surface temperature (e.g. one, two or multiple-layer approaches exist; Bonan et al. 2021) make such comparisons challenging, especially in heterogenous and topographically complex areas. Such comparisons therefore hold greater validity in a relative rather than absolute sense.

Surface temperature products from satellite sensors include MODIS Land Surface Temperature and Emissivity (daily, 1 km; Wan, Hook, and Hulley 2021), ECOSystem Spaceborne Thermal Radiometer Experiment on Space Station (ECOSTRESS) Land Surface Temperature and Emissivity (approx. 3 days, 70 m; Fisher et al. 2020), ASTER Surface Kinetic Temperature (16 days, 100 m; NASA JPL 2014), and products from Landsat instruments 4, 5, 7, 8 and 9 (16 days, 60–100 m; courtesy of US Geological Survey). The spatial and temporal coverage of these products is limited by cloud cover, however their accuracy can be relatively high and is constantly improving. An advantage of the ECOSTRESS product is the availability of images at different times of day, allowing the temporal dynamics of surface temperature to be reconstructed.

### 3.2.3. Latent heat flux

The energy associated with the transport of water from Earth's surface to the atmosphere (through evaporation, sublimation, transpiration), can be a major

component of the surface energy balance and is thus an important variable in land surface models. Although latent heat fluxes are essential e.g. for the estimation of green and white water fluxes, it is extremely difficult to measure them in a distributed way.

Several products provide ET estimates, i.e. the total amount of all vapor fluxes, for HMA (e.g. Chen et al. 2014; Fisher et al. 2020; Jung et al. 2019; Martens et al. 2017; Mu, Zhao, and Running 2011; Yuan et al. 2021; Zhang et al. 2019). Large-scale estimates of ET using satellite data usually do not distinguish between surfaces with snow and ice cover (that might experience sublimation) and those without. The ETMonitor system (1 km spatial resolution; Zheng, Jia, and Hu 2022) accounts for transient snow-covered areas and estimates sublimation using the Penman equation. Generally, ET from the ETMonitor product reproduces the expected spatial regional variation of ET, with higher ET values in the eastern and southern parts of the Tibetan Plateau and lower ET values in the central and western parts of the Tibetan Plateau (Figure 2, top left map). Other ET products, e.g. FLUXCOM (0.083° spatial resolution; e.g. Jung et al. 2019); Global Land Evaporation Amsterdam Model (GLEAM); 0.25°; e.g. Martens et al. (2017); MOD16 (MODIS Global Terrestrial Evapotranspiration Product; 500 m; e.g. Mu, Zhao, and Running 2011); EB (Surface Energy Balance Based Global Land Evapotranspiration; 0.1°; e.g. Chen et al. 2014); Penman-Monteith-Leuning Model Version 2 (PML-v2; 500 m; e.g. Zhang et al. 2019 (Figure 2), failed to capture the spatial patterns of ET in mountainous regions, despite the

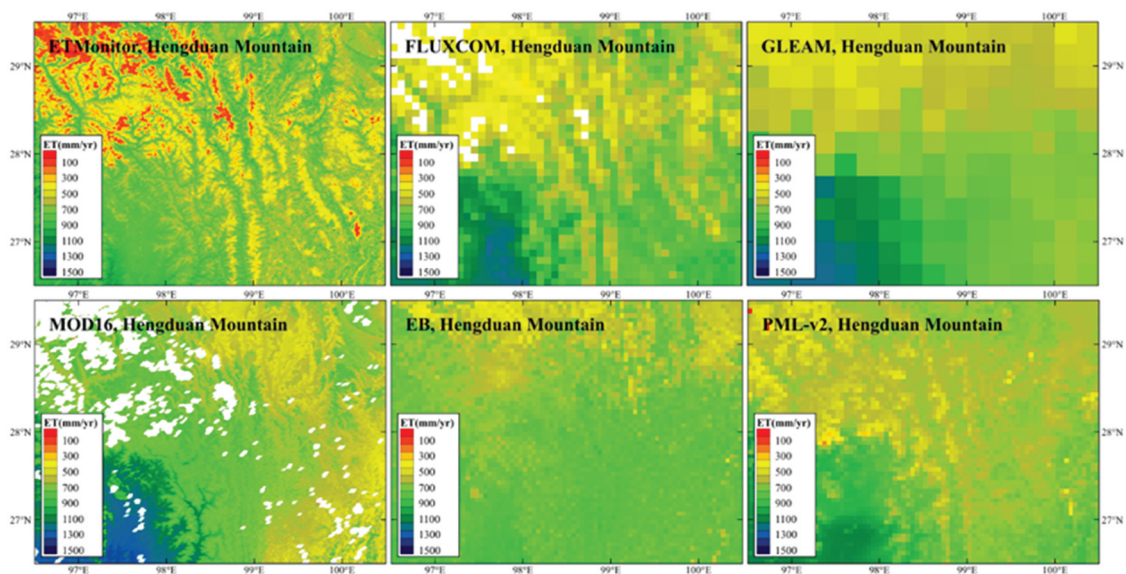


**Figure 2.** Spatial distribution of ET estimates (including sublimation where explicitly considered) from different products in the southeast edge of the Tibetan Plateau (white pixels denote “no data”): ETMonitor (1 km); FLUXCOM (0.083°); GLEAM (0.25°); MOD16 (500 m); EB (0.1°); PML-v2 (500 m).

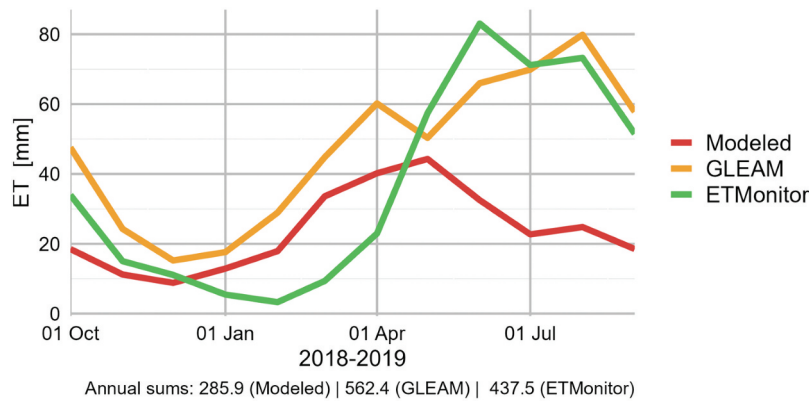


**Figure 3.** Monthly evapotranspiration amounts [mm] (including sublimation) averaged for the upper Langtang catchment for the hydrological year 2018/2019 as derived from GLEAM v3.7b (0.25° spatial resolution), ETMonitor (1 km) and modelled with T&C (100 m). Annual sums [mm] of each product are shown below the x-axis.

higher spatial resolution of some of them (MOD16 and PML-V2).

Although there are several spaceborne ET products, it is difficult to tell which is correct. A comparison of monthly averaged ET (including sublimation) over the glacierized Langtang Valley domain (Nepal), estimated based on remote sensing data (ETMonitor and GLEAM) and modeled using a mechanistic land surface model (Tethys & Chloris (T&C); Buri et al. (2023)), shows an apparent disagreement regarding subseasonal variability and annual amount of ET (Figure 3). Assuming that the modeled ET is closer to reality due to the higher spatiotemporal and physical detail and the local catchment focus of the land surface model approach, this mismatch demonstrates the need for mechanistic land surface modeling efforts in these types of catchments.

### 3.3. Hydrosphere

Estimating river discharge from remote sensing is challenging, and currently limited to rivers with low-flow cross sections wider than ~100 m (Huang et al. 2018, 2020), hindering the use of such products for most high-elevation catchments to validate simulated streamflow as a proxy for an integrated water balance component.

Distributed soil water content serves as an integrated indicator of the model's combined ability to represent subsurface soil conditions together with precipitation (amount and phase) and ET patterns. However, the currently limited spatial resolution of soil moisture products from satellite remote sensing (on the order of 0.1–1°) and difficulties in detecting water deeper in the soil (e.g. the root zone; Feldman et al. 2023; Peng et al. 2021) prevents a detailed assessment of this hydrologic component that is considered highly variable in space. Daily global soil moisture data are available from

active and passive microwave remote sensing instruments (Dorigo et al. 2017), such as the Advanced Microwave Scanning Radiometer for EOS (AMSR-E) and its successor AMSR2, the Soil Moisture and Ocean Salinity (SMOS), the Soil Moisture Active Passive (SMAP) and the Advanced Scatterometer (ASCAT) (Colliander et al. 2017; Kerr et al. 2012; Kim et al. 2015; Wagner et al. 2013). Those microwave instruments operate at different frequencies with various configurations, which can affect the sensitivity of the measurements to soil moisture. A promising approach is the multi-channel collaborative algorithm (MCCA) which can construct long-term soil moisture datasets from various satellite sensors (Zhao et al. 2021). The MCCA, in conjunction with the Zhang-Zhao's dielectric constant model (Wu et al. 2022), allows for the estimation of unfrozen water content during freezing conditions, which is important in HMA with extensive areas of permafrost and frequent freeze-thaw cycles.

## 4. Constraining and validating a land surface model with high- and moderate resolution earth observation data

In this section, we show, using results from one of the few land surface modeling studies at catchment scale, how remote sensing data can be used in a multi-step, multi-variable calibration and validation, to inform a land surface model in the simulation of blue-green-white water fluxes in a complex high elevation catchment in HMA. We use the model setup, forcing and simulations from Buri et al. (2023) to perform a set of experiments showing the potential of the new datasets from space to reduce model uncertainty, characterize processes, and then explore the partition of fluxes in the catchment.

#### 4.1. Case study description

Buri et al. (2023) simulated blue-green-white water fluxes in a high elevation 350 km<sup>2</sup> watershed in the upper Langtang Valley, Nepalese Himalayas (Figure S1), by using the state-of-the-art land surface model Tethys & Chloris (T&C; Fatichi et al. 2012a, 2012b) at a high spatio-temporal resolution (100 m, hourly). This valley was chosen due to the availability of meteorological data used to force the model, and a variety of ground-based data, used alongside the remote-sensing data for calibration and validation.

T&C models the catchment's energy- and water fluxes in a fully distributed and highly mechanistic way by resolving the surface energy balance, soil hydrology and vegetation dynamics, processes of runoff generation and flow routing, and the evolution of snow and ice packs. T&C has been applied to a large spectrum of ecosystems, environmental conditions, and scales (e.g. Botter et al. 2021; Buri et al. 2023; Fatichi et al. 2021; Fugger et al. 2022; Fyffe et al. 2021; Manoli, Ivanov, and Fatichi 2018; Mastrotheodoros et al. 2020; Paschalis et al. 2018; Shaw et al. 2022). Details about the model forcing, study catchment, model settings, and inputs can be found in Buri et al. (2023). Here, we apply the same model to show how glacier mass balance data from

space can be used to constrain the highly uncertain meteorological input data to the model, and precipitation in particular which is the main uncertainty in HMA water cycle simulations.

#### 4.2. Glacier mass balance

We leveraged a high-resolution dataset of glacier mass balance inferred from remote sensing using the continuity equation approach (Miles et al. 2021; Figure 4(b)) to constrain high elevation precipitation inputs (Figure 4(a)) in an inverse optimization approach. We forced T&C with precipitation measured at the Automatic Weather Station (AWS, Fig. S1), using seasonally variable vertical precipitation gradients (Immerzeel et al. 2014) derived from pluviometer data recorded at different sites in the study catchment. Because of a lack of high-elevation precipitation observations (>5000 m a.s.l.), the validity of a continued linear vertical gradient is questionable and a "plateau"-effect, i.e. constant or decreasing precipitation above a threshold elevation, is assumed instead (Hewitt 2005, 2011; Immerzeel, Pellicciotti, and Shrestha 2012). We tested different precipitation plateau elevations (5500, 6000, and 6500 m a.s.l.) as forcing for T&C and compared the modeled glacier mass

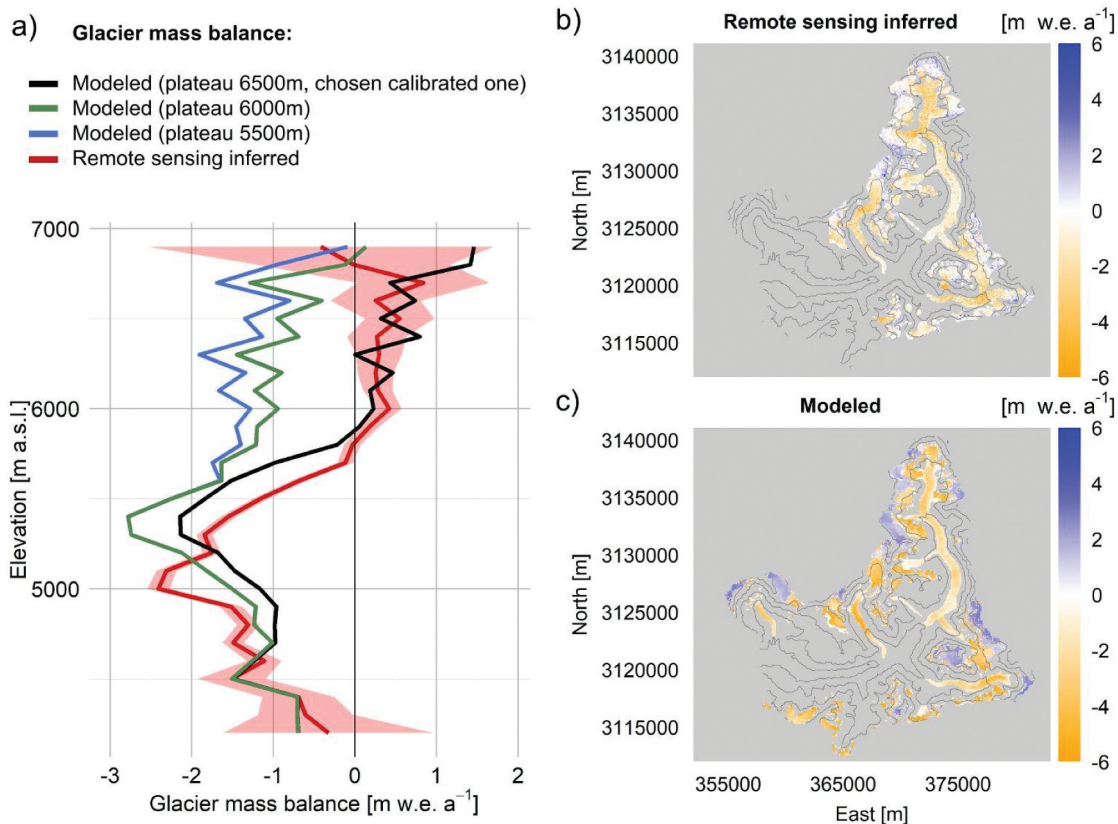


**Figure 4.** (a) Altitudinally resolved annual specific glacier mass balance for the glacierized area in the Langtang basin for the period October 2017 - October 2019 as inferred from remote sensing data based on the continuity equation approach (Miles et al. 2021) shown in red, and modelled using T&C with calibrated precipitation elevation gradients (black) and alternative precipitation gradients (blue and green, respectively). (b-c) Distributed annual glacier mass balance, inferred from remote sensing data, and modelled with T&C, respectively. Contour lines have an equidistance of 500 m.

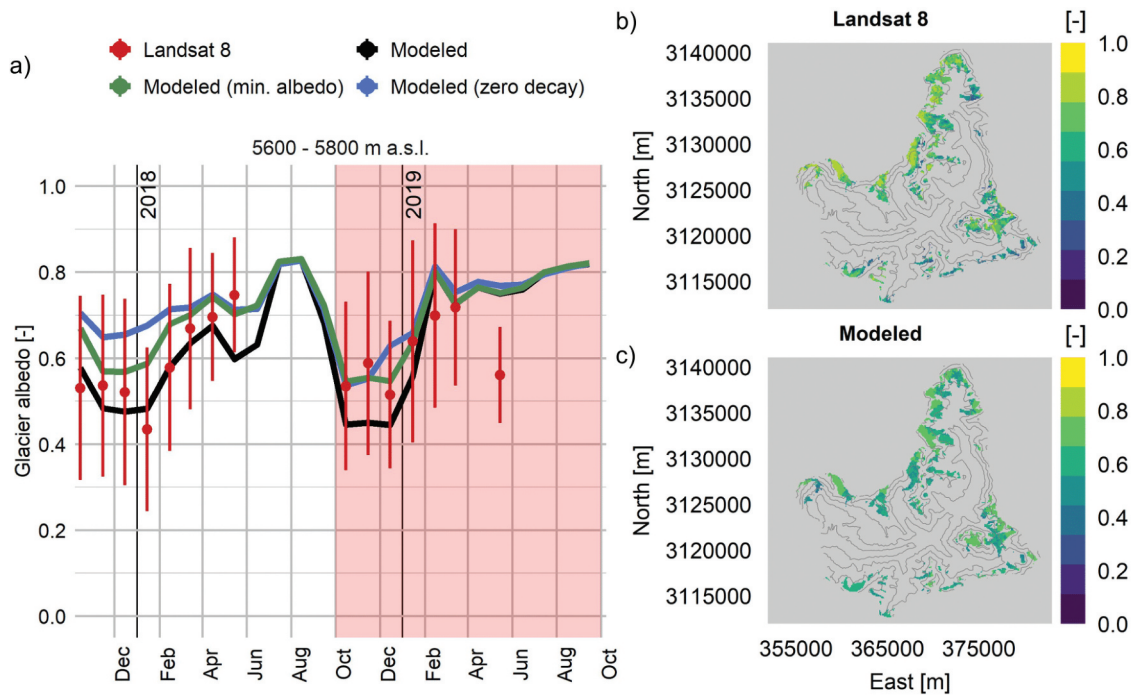


**Figure 5.** (a) Monthly averaged glacier albedos at 5600–5800 m a.s.l. in the Langtang catchment basin for the period 1 October 2017 to 30 September 2019 as observed with Landsat 8 (Ren et al. 2021) and modelled using T&C with calibrated albedo parameterizations (black) and alternative albedo parameterizations (blue and green, respectively). Main model target period (hydrological year 2018/2019 is indicated in red. (b–c) Distributed annual average glacier albedo, derived from remote sensing data, and modelled with T&C, respectively. Contour lines have an equidistance of 500 m.

balances to the remote sensing inferred estimates (Figure 4(a)). In this way, we use the highly resolved mass balance estimates from space to define the “correct” elevation of the precipitation plateau. The two lower precipitation plateaus resulted in a distinct overestimation in modeled glacier mass loss below 6000 m a.s.l. and accumulation deficit at higher elevations (blue and green lines, respectively) compared to the reference estimate (red line). Only a forcing with increasing precipitation up to 6500 m a.s.l. (black line) allowed the model to simulate sufficient accumulation rates high up (>5800 m a.s.l.) and suppressed melt rates enough in the ablation zone (<5800 m a.s.l.) of the glacierized areas in the Langtang Valley to match the glacier mass balance estimates inferred from remote sensing.

By limiting this precipitation optimization exercise to the glacierized area of the catchment, we avoid a “calibration” over the entire watershed (as often done in hydrology-oriented studies). This is important because it allows one to identify clear potential errors in precipitation inputs that could have been mistaken for errors in melt or ET if only the runoff was used to assess the correctness of the water balance.

#### 4.3. Glacier albedo

We used distributed glacier albedo observations from cloud-free Landsat 8 Operational Land Imager reflectance data (30 m spatial resolution;

courtesy of US. Geological Survey) derived with updated anisotropy parameterizations (Ren et al. 2021), to estimate the best structural bounds (adaptation to the cold high-elevation conditions) for our albedo module and to validate the evolution of glacier albedo simulated with T&C for different elevations (Figure 5(a)).

Due to the scarcity of in-situ albedo measurements at high elevations, its temporal evolution remains uncertain and snow albedo parameterizations are based on observations from lower field sites. We tested different variations based on the snow albedo parameterization of Ding et al. (2017) and show here the comparison of model results and observations for one specific elevation band (5600–5800 m a.s.l.; Figure 5(a)). At this elevation, coinciding with the current average equilibrium-line altitude of the glaciers in the Langtang Valley, we expect the highest fluctuations in glacier albedo and hence effects on melt patterns. The comparison of simulations includes three different parameterizations: i) an elevation-dependent minimum albedo with a linear increase of  $0.2 \text{ km}^{-1}$  [-], starting with 0.5 at 5500 m a.s.l. (green line); ii) a zero albedo decay under non-melting conditions (blue line); and iii) the standard run with an overall minimum snow albedo of 0.5 (black line). Although all three simulation runs were within the standard deviation of the observations (red) for the elevation band shown here (5600–5800 m a.s.l.), the standard run showed the best agreement with the observations and

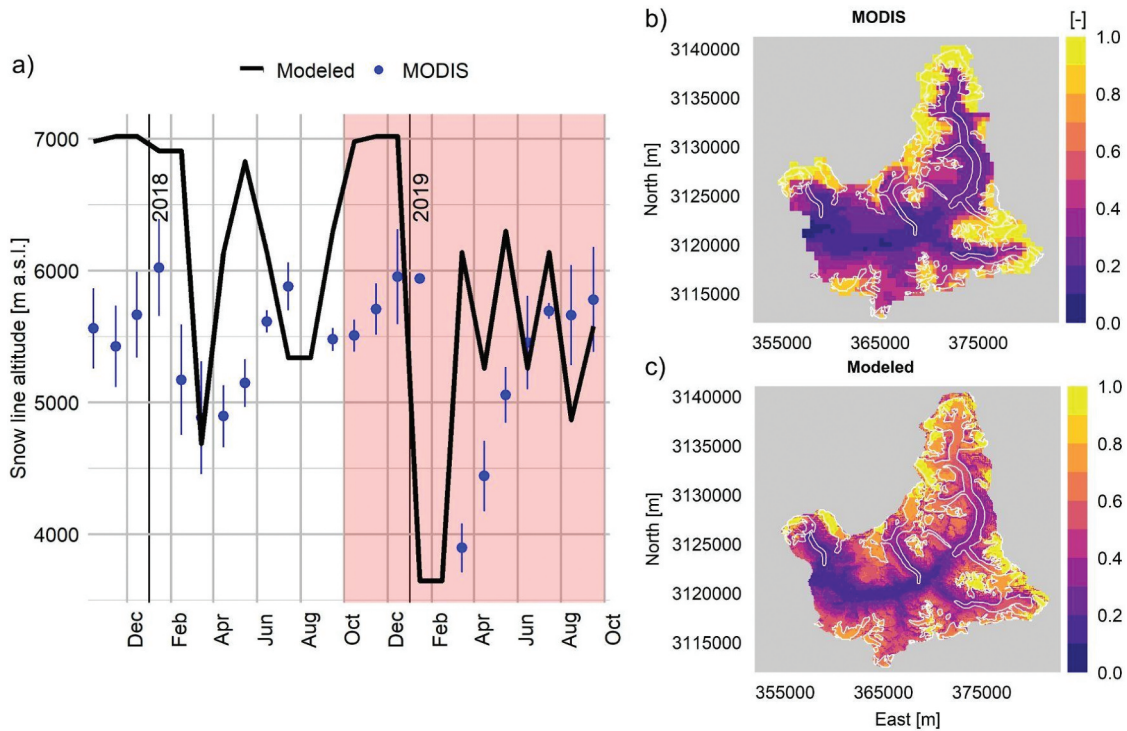


**Figure 6.** (a) Monthly averaged snow line altitudes for the upper Langtang catchment basin for the period 1 October 2017 to 30 September 2019 as observed with MODIS (MOD10A1 product from MODIS-Terra) and modelled using T&C. Main model target period (hydrological year 2018/2019 is indicated in red). (b–c) Distributed annual snow cover time fraction, derived from remote sensing data, and modelled with T&C, respectively.

was then used for the simulations of the water balance in the catchment.

Modeled annually averaged distributed glacier albedo (Figure 5) slightly underestimates glacier albedo at the highest elevations (accumulation zones) as retrieved by Landsat 8 (Figure 5(b)), but matches well the observations in the lower elevations (ablation zones). Both observed and modeled annual averages show the expected elevation gradient in albedo on glaciers.

#### 4.4. Snow cover

In contrast to glacier mass balance (Section 4.2) and glacier albedo (Section 4.3), snow cover data were not used to estimate model parameters, but to evaluate the model performance. We retrieved snow cover data (NDSI threshold: 0.4) using the daily MOD10A1 product from MODIS-Terra) (500 m spatial resolution; Hall and Riggs 2020). We compared monthly average snow-line altitudes (Figure 6(a)) observed from MODIS (blue dots) and modeled with T&C (black line). The main differences between the observed and modeled snow-line altitude are apparent in the post-monsoon season 2018 and pre-monsoon season 2019, respectively, in which the model overestimated the average snow-line altitude in the catchment, i.e. the model simulated a smaller snow cover fraction in the catchment with an earlier snow pack depletion at low elevations in both shoulder seasons (spring and autumn). The modeled

annually averaged distributed snow cover fraction (Figure 6(c)) shows a smaller area with permanent snow cover (snow cover time fraction = 1) than retrieved by MODIS (Figure 6(b)). However, the simulations show more gradual changes in annual snow cover with elevation compared to MODIS, which might indicate some limitations related to the coarse spatial resolution of the satellite product.

#### 4.5. Leaf Area Index

We used LAI to evaluate the performance of T&C regarding vegetation dynamics, which has rarely been considered in high elevation catchments, to the best of our knowledge. We extracted LAI from the VNP15A2H product from the VIIRS instrument on board the Suomi-National Polar-orbiting Partnership (S-NPP; 500 m spatial resolution; Myneni and Knyazkhin 2018) and MODIS (MCD15A3H, Terra + Aqua combined 4 day repeat cycle; 500 m spatial resolution). We discarded pixels that were recorded with low quality regarding clouds, cloud shadows, high aerosol quantity, and snow, respectively, and then compared the cleaned LAI to the spatially averaged T&C model outputs for all pixels assigned with larch vegetation (Figure 7(a); see Figure S2 for distribution of larch vegetation). Simulated and observed LAIs for larch agree relatively well in the growing phase in pre-monsoon 2019, whereas the satellite products estimate decreasing LAI earlier in the post-monsoon than the

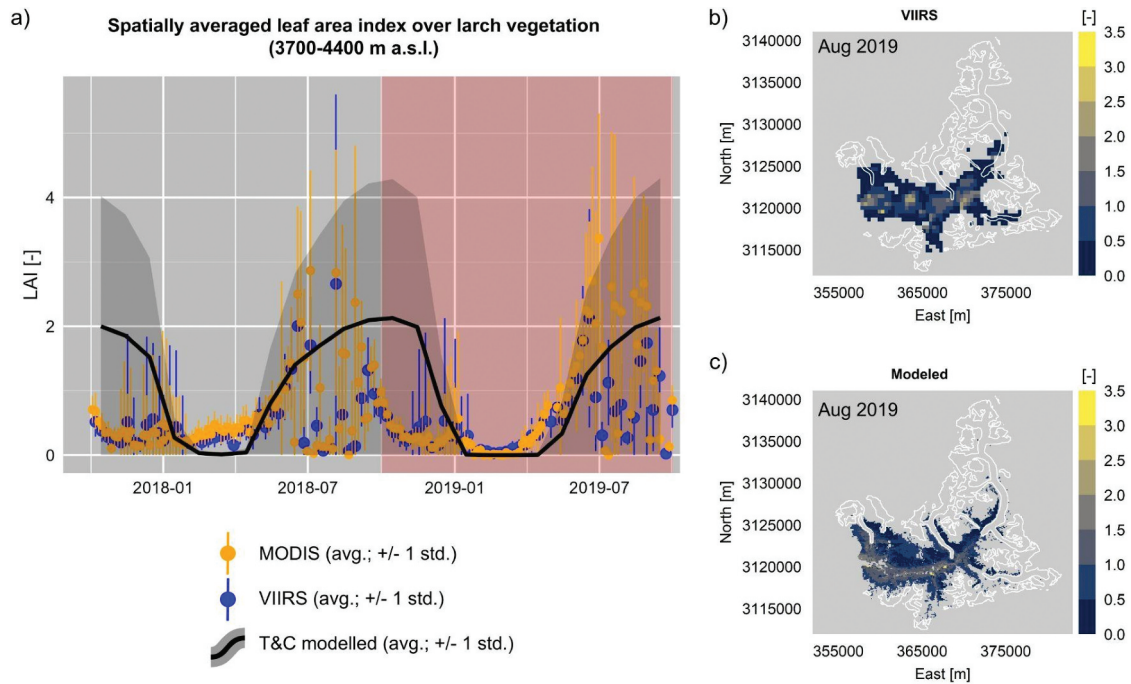


**Figure 7.** (a) Spatially averaged Leaf Area Indices for larch vegetation in the upper Langtang catchment basin for the period 1 October 2017 to 30 September 2019 as observed (with MODIS and VIIRS, respectively) and modelled using T&C (monthly average). Main model target period (hydrological year 2018/2019 is indicated in red. (b–c) Distributed average LAI for August 2019 as an example snapshot covering the entire watershed, derived from remote sensing data (VIIRS) and modelled with T&C, respectively. White lines indicate glaciers.

model. This discrepancy could be due to the patchy occurrence of larch stands in the study catchment, which is not reflected well by the coarse remote sensing products. The influence of spatial resolution on the general pattern can also be seen in the annually averaged maps, where the simulated LAIs (Figure 7(c)) follow a more gradual and potentially more realistic pattern with topography and land cover than the satellite product (Figure 7(b)). Moreover, general uncertainties in modeled and remotely sensed LAI values reveal the need for more vegetation-specific ground observations, e.g. through phenological cameras (Brown et al. 2016).

#### 4.6. Land surface temperature

T&C simulates surface temperature by resolving the energy balance and this variable is thus an important indicator for the model performance regarding energy fluxes in general and latent heat in particular. The ECOSTRESS product provides land surface temperature at a spatial resolution of ~65 m (Fisher et al. 2020) and since its installation in July 2018 it passed over the study region approximately at a 3-day frequency. However, due to cloud cover or incomplete coverage, only 17% of the available imagery (8 of 47 images during the target period) were usable to retrieve the surface temperature across the watershed. We compared the remote sensing derived land surface temperatures, spatially averaged over all debris-covered

ice pixels in the study catchment (see Figure S1 for distribution of debris covered ice) for each satellite overpass, with the simulated surface temperatures (Figure 8(a)). The observed surface temperatures (dots) were captured by the model (line) at different hours of the day (dot colors). Figure 8(b) shows the direct comparison of modeled and observed surface temperatures at the AWS-site for different days of the year (dot colors).

Nevertheless, direct comparisons of observed and modeled surface temperatures, especially in complex catchments, are challenging (see also Surface temperature in Section 3.2.2 above) and should be assessed in a relative rather than absolute sense.

## 5. Discussion

### 5.1. Insights into blue-green-white water fluxes' partition

Distributed results from the T&C simulations (Figure 9) show the complex feedbacks between topography, elevation, and land cover and reveal the importance of applying a detailed mechanistic model to unravel all these interactions.

At the annual scale (hydrological year 2018/2019) the domain's water fluxes in the Langtang Valley amount to 1210 mm (blue), 122 mm (green), and 164 mm (white), respectively (Table 1 in Buri et al. 2023). Evaporation and sublimation (E) are important in the catchment, occurring on most of the land

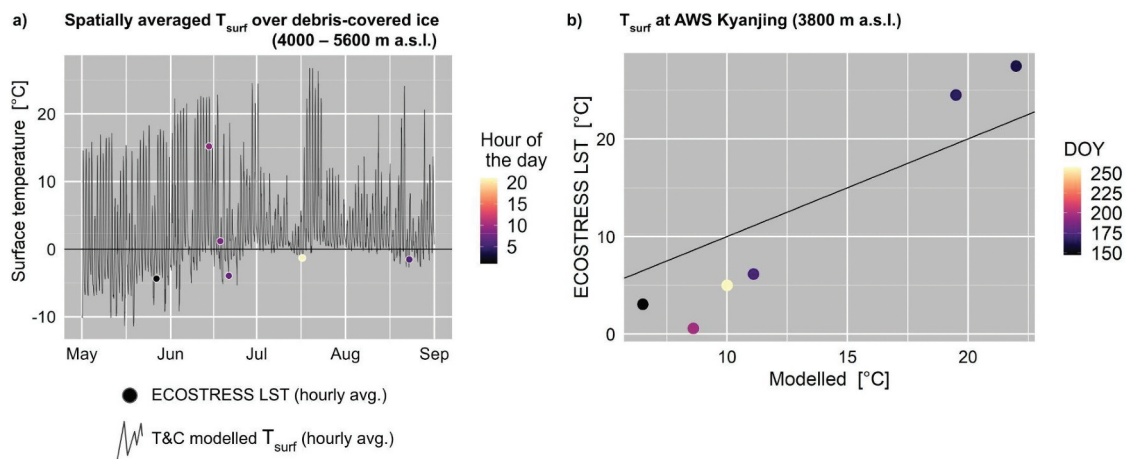


**Figure 8.** (a) Spatially averaged hourly surface temperature for all debris-covered ice in the Langtang Valley for the period May to September 2019, as modelled with T&C (line) and derived from ECOSTRESS product (dots). Dot colour indicates hour of the day of satellite product acquisition. (b) Modelled against ECOSTRESS surface temperature at Kyanjing automatic weather station for points in time with matching ECOSTRESS spatiotemporal coverage. Dot colour indicates day of the year.

surfaces except the rock and supraglacial debris surfaces when they are snow free (Figure 9(a)), summing up to a catchment total of 260 mm w.e.  $a^{-1}$  (Buri et al. 2023). Simulating dynamic subsurface soil conditions (e.g. infiltration and lateral flow routing) is especially important in the summer months (April – September), with very high spatial variability in  $E$  (Figure 9(a)), mainly through evaporation from the ground and standing water (Figures S3-S4).

Transpiration Rates ( $T_r$ ; Figure 9(b)) are highest during monsoon, coinciding with a peak productivity through generally higher temperatures and vapor pressure deficits. Evaporation from intercepted water on vegetation ( $E_{intercept.,veg.}$ ; Figure 9(c)) shows a clear peak during the monsoon season (July – September), and a clear vertical gradient controlled by air temperature (see Figure S5 for modeled mean annual air temperature). The vapor lost to the atmosphere from snow and ice surfaces (white water, primarily sublimation;  $E_{snow/ice}$ ; Figure 9(d)) only happens in very high elevations of the study basin (>6500 m) throughout the year in considerable amounts. Only in winter (January – March) when snow covers large parts of the catchment and atmospheric conditions are cold and dry enough  $E_{snow/ice}$  takes place in most of the Langtang Valley. We simulated substantial sublimation rates at high elevations during the winter season (0.6, 0.7, and 1.3 mm  $d^{-1}$  at 5000, 6000, and 7000 m a. s.l., respectively, from January to March) and in spring (0.5, 1.3, and 1.6 mm  $d^{-1}$  at 5000, 6000, and 7000 m a. s.l., respectively, from April to June).

The ET/precipitation ratio (ET as total evapotranspiration, including sublimation; precipitation as total solid and liquid precipitation; Figure 10(a)) at the annual scale shows a clear vertical gradient. It demonstrates the relevance of green water fluxes and in particular vegetation (through transpiration and evaporation from interception; Figure 9(b-c)) for the water balance

in the lowest zones of the study catchment. However, the ratio of the total water lost to the atmosphere (ET) to the sum of all direct contributions of liquid water (rain, snow melt and ice melt; Figure 10(b)) reveals how important green and white water fluxes are compared to blue water amounts in a spatial dimension. Our simulations show that at high elevations sublimation is the only energy flux that removes water from areas covered by snow and ice, as snow and ice melt are shut down, which is in agreement with recent observation-based considerations of glacier mass balance e.g. on Everest's South Col Glacier (Brun et al. 2022; Potocki et al. 2022). Our simulations reveal in a distributed way the important role of sublimation at high altitudes and in the winter season, which has been observed at the point scale (Litt et al. 2019; Sherpa et al. 2023; Stigter et al. 2018; Wagnon et al. 2013) but never quantified for an entire catchment.

## 5.2. Remaining challenges and pathways forward

In this article, we have updated the definition of blue and green water fluxes and provided an example of modeling the cryo-hydro-biosphere continuum in high mountain catchments and we showed how considering the interactions between spheres is important (Section 2). We have discussed recent developments in spaceborne Earth observation products that have the potential to support catchment modeling in high mountain regions (Section 3) and presented a promising pilot study application of the mechanistic land surface model T&C to a glacierized Himalayan basin and explain the use of high-resolution Earth observation data to constrain the meteorological uncertainty and validate our model results (Section 4). Here, we use the lessons learnt to highlight the remaining challenges and future opportunities that



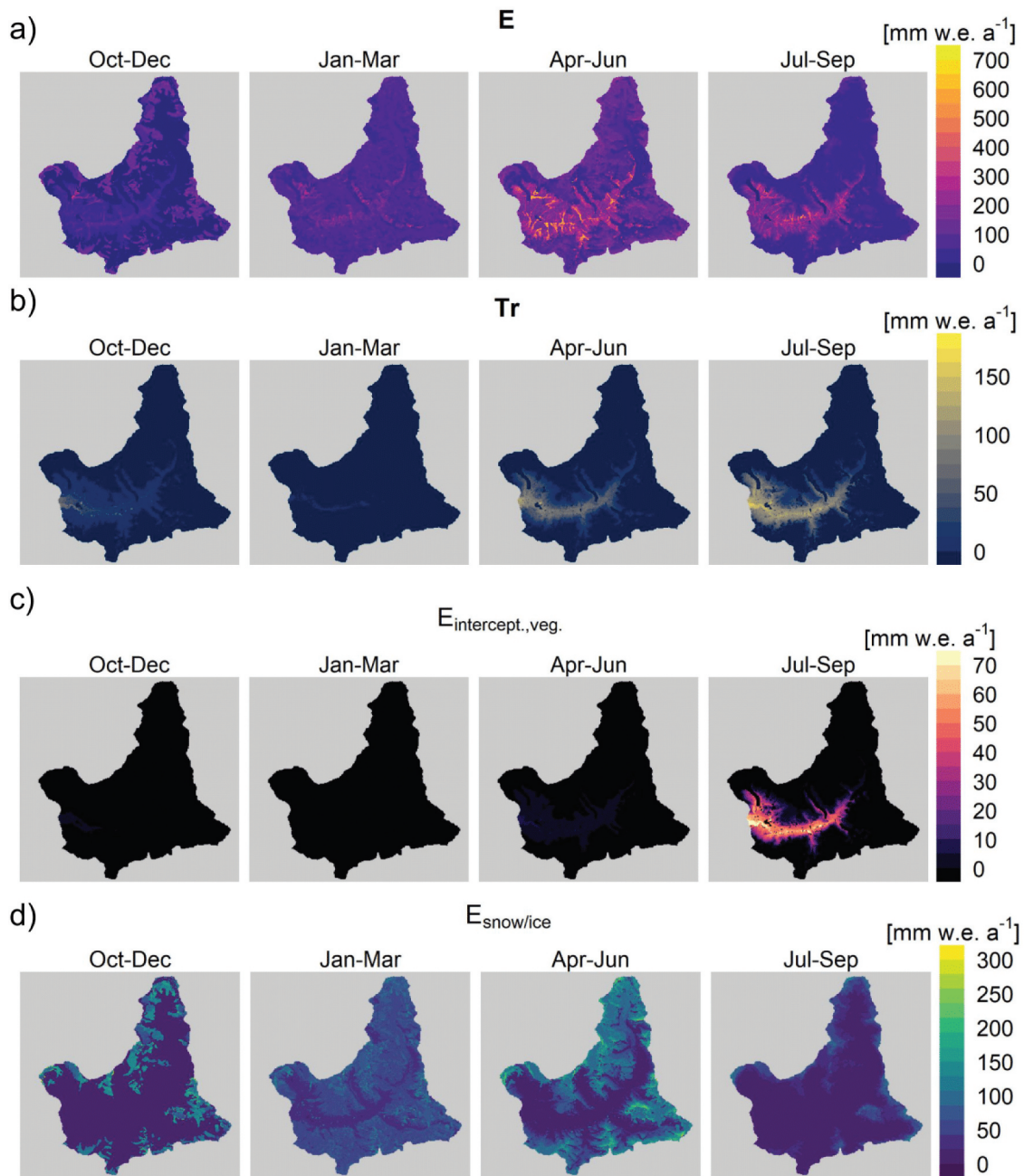


**Figure 9.** Distributed quarter-annual sums of (a) total evaporation ( $E$ ; evaporation and sublimation, without plant transpiration), (b) plant transpiration ( $Tr$ ), (c) evaporation from vegetation-interception ( $E_{intercept.,veg.}$ ), and (d) sublimation from snow and ice ( $E_{snow/ice}$ ).

remote sensing data presents for land surface modeling in HMA.

### 5.2.1. Remote sensing products for modellers

Developments in processing and storing spaceborne Earth observation data in recent years brought a massive transition from custom workflows, i.e. needing a specialist for every application, to operationally available near real-time data in various fields of environmental research. For the cryosphere and hydrosphere, datasets of glacier thinning (Hugonnet et al. 2021), glacier surface motion (Millan et al. 2023), glacier/snow albedo and snow cover area (MODIS), land surface temperature (Landsat TM; ECOSTRESS), ET

(ECOSTRESS; Fisher et al. 2020) and vegetation indices (MODIS) are now operationally available. Besides the open-data policy associated with an increasing number of remote-sensing products, powerful platforms (e.g. cloud computing services) that allow easy and timely access to these datasets are an essential tool that improved the usability of remote sensing products in recent years, e.g. Google Earth Engine, AppEEARS, Microsoft Planetary Computer, SentinelHub and others. To further ease the use of earth observation data for validation and evaluation in land surface models new remote sensing studies should use these platforms in order to allow more easily reproducible workflows for modelers.

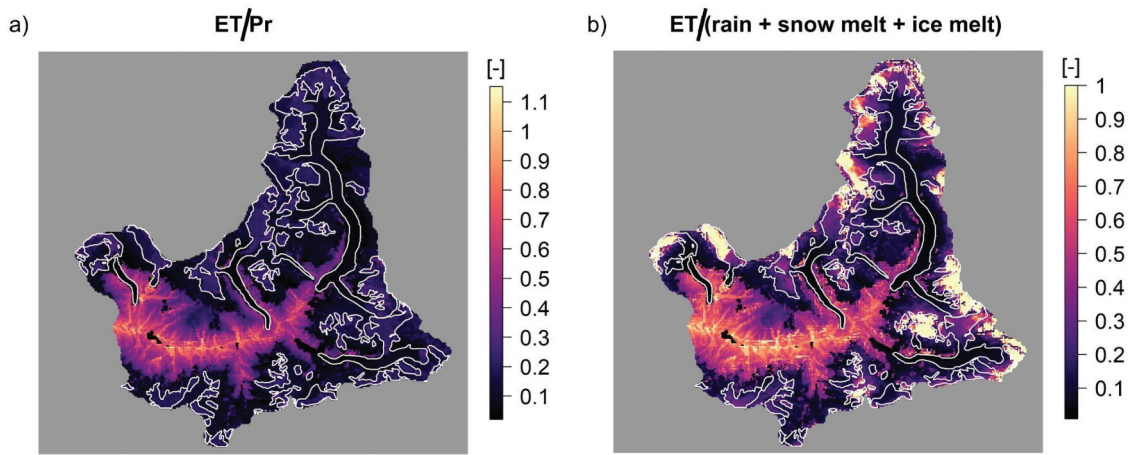


**Figure 10.** Maps of total annual per-pixel ratio of (a) ET (including sublimation) divided by (liquid and solid) precipitation and (b) ET (including sublimation) divided by the sum of rain, snow melt and ice melt for the upper Langtang catchment (hydrological year 2019), modelled with T&C. Glacier outlines are shown in white.

### 5.2.2. Water balance components hidden from satellites

Despite the extraordinary progress in the ability of remote-sensing products to provide individual water balance components, many key variables remain challenging or impossible to monitor. Satellite-derived estimates of precipitation can vary widely due to the specific sensors utilized and the relationships between predictors and precipitation, as well as bias-correction and blending methodologies (a detailed overview is provided by Sun et al. 2018). Here, we have highlighted the potential of process-based models to back-compute the magnitude and timing of precipitation at extreme elevations based upon glacier mass balance, a very promising way forward which however cannot provide sub-seasonal variability and interannual fluctuations, unless satellite derived glacier mass balance products become available at those resolutions. ET is a second key variable that remains largely elusive, and difficult to constrain. Although a variety of spaceborne ET products exist, these are not direct observations but modeled quantities or parameterized indirectly based on various data sources (Figure 2). Most of these products are constrained by coarse spatial resolution, low overpass-frequencies, and quality issues related to cloud cover. Therefore, simulated latent heat fluxes are extremely challenging to validate with remote-sensing data. There is also a lack of eddy-covariance measurements in high mountain regions, and so their installation – in locations where topography allows – in underrepresented land covers, climatic regimes, and elevations in HMA would be beneficial to improve the validation of both land surface models and remote sensing products.

Groundwater is a largely unconstrained water balance component. It is impractical to be assessed from space in complex mountain terrain. Estimates of

groundwater changes using spaceborne gravimetry measurements (Gravity Recovery and Climate Experiment, GRACE) exist at the regional scale (Jacob et al. 2012; Loomis et al. 2019; Scanlon et al. 2018), but are too coarse (>100 km spatial resolution) to capture changes in the terrestrial water storage in individual mountain watersheds.

### 5.2.3. Future developments in land surface modelling

Expanding cloud computing resources (and the advent of machine learning) will likely modify the field significantly, with land surface models able to run much faster and which will likely have data-driven components combined with process-based components (e.g. Zhao et al. 2019). This will allow their application at both high or hyper spatial resolution and on a very large spatial scale, a challenge in present conditions. The increasing availability and resolution of remote sensing products can help substantially in both informing and constraining complex land surface models. Probably for the first time in the era of spaceborne Earth observation the spatial resolution of remote sensing data starts to be interesting for mechanistic approaches that simulate the cryosphere-hydrosphere-biosphere continuum at high spatiotemporal resolution, which will give them a boost in the coming decade.

However, issues regarding complex topography remain, and whereas many processes and states at the land surface can be retrieved (e.g. snow, ice, vegetation, and temperature), their quality over complex terrains remains to be further evaluated. Additionally, the below-ground remains completely hidden from space. Subsurface conditions are extremely heterogeneous and, to date, not even the simplest boundary condition (e.g. soil depth), although important for many processes, is known beyond the plot scale. Belowground

characteristics can only be estimated indirectly (e.g. Stocker et al. 2023) or by analyzing properties of hydrographs (e.g. Beck et al. 2013; Cooper et al. 2023), or can be approximated by stochastic approaches that are informed with the statistical properties of the subsurface heterogeneity (e.g. Maxwell and Kollet 2008), which are presently unconstrained. This will be one of the next frontiers for remote sensing applied to the cryo- and hydrosphere.

The main benefit of the projected advancements in mechanistic high-resolution land surface modeling will be to have results which are “physically constrained”, concurrently for all variables: no other approach – not even direct observations – can produce such results, which are distributed, i.e. that every point matters, with the clear capability to run scenarios where the complexity of and nonlinear relationships between the water cycle and ecological components is preserved.

### Disclosure statement

No potential conflict of interest was reported by the author(s).

### Funding

This work was supported by the ESA and NRSCC Dragon 5 cooperation project “Cryosphere-hydrosphere interactions of the Asian water towers: using remote sensing to drive hyper-resolution ecohydrological modelling” [Grant no. 59199]. PB and FP acknowledge funding from the SNSF (High-elevation precipitation in High Mountain Asia, HOPE) [Grant no. 183633]. ESM, MK, SFu and FP acknowledge funding from the ERC under the European Union’s Horizon 2020 research and innovation program (Rapid mass losses of debris-covered glaciers in High Mountain Asia, RAVEN) [Grant no. 772751]. LJ, CZ and MMe acknowledge the Second Tibetan Plateau Scientific Expedition and Research Program (STEP) [grant no. 2019QZKK010308, no. 2019QZKK0206], the National Natural Science Foundation of China projects (Grant no. 42171039, no. 91737205), the Chinese Academy of Sciences President’s International Fellowship Initiative [Grant no. 2020VTA0001], and the MOST High-Level Foreign Expert Program [Grant no. G2022055010L].

### Notes on contributors

**Pascal Buri** is a research scientist at the Swiss Federal Research Institute WSL. His research interests include the cryosphere and ecohydrology of high mountain regions, which he investigates through numerical modeling, combining field data and remote sensing products.

**Simone Fatichi** is an Associate Professor in the Department of Civil and Environmental Engineering at the National University of Singapore. His research interests include how global change impacts vegetation functioning, water, and soil resources, carbon cycle, and ecosystem services in natural and urban environments.

**Thomas Shaw** is a postdoctoral researcher at the Institute of Science and Technology Austria. His research interests revolve around cryosphere–atmosphere interactions and the downscaling and estimation of meteorology in high mountain regions.

**Catriona Fyffe** is a postdoctoral researcher at the Institute of Science and Technology Austria. She is a glacier-hydrologist with interests in debris-covered and tropical glaciers and their role in high mountain catchment hydrology.

**Evan Miles** is a research scientist at the Swiss Federal Research Institute WSL. He is a glaciologist and hydrologist focused on developing new observations to understand glacier-climate processes and hydrology, particularly in High Mountain Asia.

**Michael McCarthy** is a research scientist at the Swiss Federal Research Institute WSL. His research focuses on how mountain regions respond to climate change and hydroclimatic extremes.

**Marin Kneib** is a postdoctoral researcher at the Institute of Environmental Geosciences in Grenoble and at the Department of Atmospheric and Cryospheric Sciences of University of Innsbruck. His research focuses on the evolution of the cryosphere in a changing climate, from the local to the regional scale.

**Shaoting Ren** is a postdoctoral researcher at the Swiss Federal Research Institute WSL. He is a glacio-hydrologist with interests in the evolution of glaciers in High Mountain Asia by remote sensing and modeling.

**Achille Jouberton** is a doctoral student at the Swiss Federal Institute for Forest, Snow and Landscape Research (WSL) and at the Swiss Federal Institute of Technology in Zurich (ETH). He is a glacio-hydrologist with interests in glacier mass changes and snow accumulation dynamics in High Mountain Asia.

**Stefan Fugger** is a doctoral student at the Institute of Science and Technology Austria (ISTA), the Swiss Federal Institute for Forest, Snow, and Landscape Research (WSL), and the Swiss Federal Institute of Technology in Zürich (ETH Zürich). His research is focussing on the hydrology of high-elevation catchments via mechanistic numerical modeling, remote sensing and field work.

**Li Jia** is a leading scientist in Earth observation for terrestrial water cycle, water resource and climate change at Aerospace Information Research Institute, Chinese Academy of Sciences. She is currently a member of the GEWEX-GHP (Global Energy and Water Exchanges program-Hydroclimatology Panel).

**Jing Zhang** is currently a postdoctoral researcher at the National Space Science Center of the Chinese Academy of Sciences. Her research interests include glacier surface velocity extraction, glacier mass balance, and glacier dynamic modeling.

**Cong Shen** is a master student at the Aerospace Information Research Institute, Chinese Academy of Sciences, China. His research interests include glacier surface elevation extraction, and glacier mass balance.

**Chaolei Zheng** is an Associate Professor at the Aerospace Information Research Institute, Chinese Academy of Sciences, China. His research interests include the

remote sensing-based modeling and monitoring of evapotranspiration, soil moisture downscaling, global water resource products development and application.

**Massimo Menenti** held senior research positions in The Netherlands, France, USA, China and Italy. His best-known achievements have been attained in the aspects of surface parameter retrievals from remote sensing, remote sensing-based evapotranspiration estimation and the application of remote sensing technology in hydrology and climate models.

**Francesca Pellicciotti** is a Professor at the Institute of Science and Technology Austria. She uses models to study the interactions of climate and glaciers, snow, and water resources, to understand the role of the mountain cryosphere in a changing world, going from single glaciers to entire mountain regions.

## References

- Armstrong, R. L., K. Rittger, M. J. Brodzik, A. Racoviteanu, A. P. Barrett, S. J. S. Khalsa, B. Raup, et al. 2019. "Runoff from Glacier Ice and Seasonal Snow in High Asia: Separating Melt Water Sources in River Flow." *Regional Environmental Change* 19 (5): 1249–1261. <https://doi.org/10.1007/s10113-018-1429-0>.
- Bandyopadhyay, J., D. Kraemer, R. Kattelmann, and Z. W. Kundzewicz. 1997. "Highland waters: A resource of global significance." In *Mountains of the World: A Global Priority*, edited by B. Messerli and J. Ives, 131–155. New York: Parthenon.
- Beck, H. E., A. I. J. M. Van Dijk, D. G. Miralles, R. A. M. De Jeu, L. A. Bruijnzeel, T. R. Mcvicar, and J. Schellekens. 2013. "Global Patterns in Base Flow Index and Recession Based on Streamflow Observations from 3394 Catchments." *Water Resources Research* 49 (12): 7843–7863. <https://doi.org/10.1002/2013WR013918>.
- Berthier, E., D. Floriciou, A. S. Gardner, N. Gourmelen, L. Jakob, F. Paul, D. Treichler, et al. 2023. "Measuring Glacier Mass Changes from Space—A Review." *Reports on Progress in Physics* 86 (3): 36801. <https://doi.org/10.1088/1361-6633/acaf8e>.
- Bhattacharya, A., T. Bolch, K. K. Mukherjee, O. Menounos, B. Kapitsa, V. Neckel, N. Yang, et al. 2021. "High Mountain Asian Glacier Response to Climate Revealed by Multi-Temporal Satellite Observations Since the 1960s." *Nature Communications* 12: 4133. <https://doi.org/10.1038/s41467-021-24180-y>.
- Bierkens, M. F. P., V. A. Bell, P. Burek, N. Chaney, L. E. Condon, C. H. David, A. De Roo, et al. 2015. "Hyper-Resolution Global Hydrological Modelling: What Is Next?" *Hydrological Processes* 29 (2): 310–320. <https://doi.org/10.1002/hyp.10391>.
- Blyth, E. M., V. K. Arora, D. B. Clark, S. J. Dadson, M. G. De Kauwe, D. M. Lawrence, J. R. Melton, et al. 2021. "Advances in Land Surface Modelling." *Current Climate Change Reports* 7 (2): 45–71. <https://doi.org/10.1007/s40641-021-00171-5>.
- Bonan, G. B., E. G. Patton, J. J. Finnigan, D. D. Baldocchi, and I. N. Harman. 2021. "Moving Beyond the Incorrect but Useful Paradigm: Reevaluating Big-Leaf and Multilayer Plant Canopies to Model Biosphere-Atmosphere Fluxes – A Review." *Agricultural and Forest Meteorology* 306:108435. <https://doi.org/10.1016/j.agrfor.2021.108435>.
- Botter, M., M. Zeeman, P. Burlando, and S. Fatichi. 2021. "Impacts of Fertilization on Grassland Productivity and Water Quality Across the European Alps Under Current and Warming Climate: Insights from a Mechanistic Model." *Biogeosciences* 18 (6): 1917–1939. <https://doi.org/10.5194/bg-18-1917-2021>.
- Brown, T. B., K. R. Hultine, H. Steltzer, E. G. Denny, M. W. Denslow, J. Granados, S. Henderson, et al. 2016. "Using Phenocams to Monitor Our Changing Earth: Toward a Global Phenocam Network." *Frontiers in Ecology and the Environment* 14 (2): 84–93. <https://doi.org/10.1002/fee.1222>.
- Brun, F., O. King, M. Réveillet, C. Amory, A. Planchot, E. Berthier, A. Dehecq, et al. 2022. "Brief communication: Everest South Col Glacier Did Not Thin During the Last Three Decades." *The Cryosphere Discussions* 1–27. <https://doi.org/10.5194/tc-2022-166>.
- Buri, P., S. Fatichi, T. E. Shaw, E. S. Miles, M. J. McCarthy, C. L. Fyffe, S. Fugger, et al. 2023. "Land Surface Modeling in the Himalayas: On the Importance of Evaporative Fluxes for the Water Balance of a High-Elevation Catchment." *Water Resources Research* 59 (10): e2022WR033841. <https://doi.org/10.1029/2022WR033841>.
- Buri, P., E. S. Miles, J. F. Steiner, S. Ragetti, and F. Pellicciotti. 2021. "Supraglacial Ice Cliffs Can Substantially Increase the Mass Loss of Debris-Covered Glaciers." *Geophysical Research Letters* 48 (6): e2020GL092150. <https://doi.org/10.1029/2020GL092150>.
- Carnahan, E., J. M. Amundson, and E. Hood. 2019. "Impact of Glacier Loss and Vegetation Succession on Annual Basin Runoff." *Hydrology and Earth System Sciences* 23 (3): 1667–1681. <https://doi.org/10.5194/hess-23-1667-2019>.
- Cauvy-Fraunié, S., and O. Dangles. 2019. "A Global Synthesis of Biodiversity Responses to Glacier Retreat." *Nature Ecology & Evolution* 3 (12): 1675–1685. <https://doi.org/10.1038/s41559-019-1042-8>.
- Chen, J. M., and T. A. Black. 1992. "Defining Leaf Area Index For Non-Flat Leaves." *Plant, Cell & Environment* 15 (4): 421–429. <https://doi.org/10.1111/j.1365-3040.1992.tb00992.x>.
- Chen, X., Z. Su, Y. Ma, S. Liu, Q. Yu, and Z. Xu. 2014. "Development of a 10-Year (2001–2010) 0.1° Data Set of Land-Surface Energy Balance for Mainland China." *Atmospheric Chemistry & Physics* 14 (23): 13097–13117. <https://doi.org/10.5194/acp-14-13097-2014>.
- Clark, D. B., L. M. Mercado, S. Sitch, C. D. Jones, N. Gedney, M. J. Best, M. Pryor, et al. 2011. "The Joint UK Land Environment Simulator (Jules), Model Description – Part 2: Carbon Fluxes and Vegetation Dynamics." *Geoscientific Model Development* 4 (3): 701–722. <https://doi.org/10.5194/gmd-4-701-2011>.
- Cogley, J. G. 2011. "Present and Future States of Himalaya and Karakoram Glaciers." *Annals of Glaciology* 52 (59): 69–73. <https://doi.org/10.3189/172756411799096277>.
- Colliander, A., T. J. Jackson, R. Bindlish, S. Chan, N. Das, S. B. Kim, M. H. Cosh, et al. 2017. "Validation of SMAP Surface Soil Moisture Products with Core Validation Sites." *Remote Sensing of Environment* 191:215–231. <https://doi.org/10.1016/j.rse.2017.01.021>.
- Cooper, M. G., T. Zhou, K. E. Bennett, W. R. Bolton, E. T. Coon, S. W. Fleming, J. C. Rowland, and J. Schwenk. 2023. "Detecting Permafrost Active Layer Thickness Change from Nonlinear Baseflow Recession." *Water Resources Research* 59 (1): e2022WR033154. <https://doi.org/10.1029/2022WR033154>.

- Dehecq, A., A. S. Gardner, O. Alexandrov, S. Mcmichael, R. Hugonnet, D. Shean, and M. Marty. 2020. "Automated Processing of Declassified KH-9 Hexagon Satellite Images for Global Elevation Change Analysis Since the 1970s." *Frontiers in Earth Science* 8. <https://doi.org/10.3389/feart.2020.566802>.
- Dehecq, A., N. Gourmelen, A. S. Gardner, F. Brun, D. Goldberg, P. W. Nienow, E. Berthier, et al. 2019. "Twenty-First Century Glacier Slowdown Driven by Mass Loss in High Mountain Asia." *Nature Geoscience* 12 (1): 22–27. <https://doi.org/10.1038/s41561-018-0271-9>.
- De Kauwe, M. G., S. X. Zhou, B. E. Medlyn, A. J. Pitman, Y. P. Wang, R. A. Duursma, and I. C. Prentice. 2015. "Do Land Surface Models Need to Include Differential Plant Species Responses to Drought? Examining Model Predictions Across a Mesic-Xeric Gradient in Europe." *Biogeosciences* 12 (24): 7503–7518. <https://doi.org/10.5194/bg-12-7503-2015>.
- De Kok, R. J., O. A. Tuinenburg, P. N. J. Bonekamp, and W. W. Immerzeel. 2018. "Irrigation As a Potential Driver for Anomalous Glacier Behavior in High Mountain Asia." *Geophysical Research Letters* 45 (4): 2047–2054. <https://doi.org/10.1002/2017GL076158>.
- Ding, B., K. Yang, W. Yang, X. He, Y. Chen, X. G. Lazhu, L. Wang, et al. 2017. "Development of a Water and Enthalpy Budget-Based Glacier Mass Balance Model (WEB-GM) and Its Preliminary Validation." *Water Resources Research* 53 (4): 3146–3178. <https://doi.org/10.1002/2016WR018865>.
- Dorigo, W., W. Wagner, C. Albergel, F. Albrecht, G. Balsamo, L. Brocca, D. Chung, et al. 2017. "ESA CCI Soil Moisture for Improved Earth System Understanding: State-Of-The Art and Future Directions." *Remote Sensing of Environment* 203:185–215. <https://doi.org/10.1016/j.rse.2017.07.001>.
- Falkenmark, M. 1995. "Coping with Water Scarcity Under Rapid Population Growth." Conference of SADC Ministers, Pretoria, August 25–26.
- Falkenmark, M., and J. Rockström. 2006. "The New Blue and Green Water Paradigm: Breaking New Ground for Water Resources Planning and Management." *Journal of Water Resources Planning and Management* 132 (3): 129–132. [https://doi.org/10.1061/\(ASCE\)0733-9496\(2006\)132:3\(129\)](https://doi.org/10.1061/(ASCE)0733-9496(2006)132:3(129)).
- Fan, Y., M. Clark, D. M. Lawrence, S. Swenson, L. E. Band, S. L. Brantley, and D. Yamazaki. 2019. "Hillslope Hydrology in Global Change Research and Earth System Modeling." *Water Resources Research* 55 (2): 1737–1772. <https://doi.org/10.1029/2018WR023903>.
- Fang, H., F. Baret, S. Plummer, and G. Schaepman-Strub. 2019. "An Overview of Global Leaf Area Index (LAI): Methods, Products, Validation, and Applications." *Reviews of Geophysics* 57 (3): 739–799. <https://doi.org/10.1029/2018RG000608>.
- Farinotti, D., M. Huss, J. J. Fürst, J. Landmann, H. Machguth, F. Maussion, and A. Pandit. 2019. "A Consensus Estimate for the Ice Thickness Distribution of All Glaciers on Earth." *Nature Geoscience* 12 (3): 168–173. <https://doi.org/10.1038/s41561-019-0300-3>.
- Fatichi, S., V. Y. Ivanov, and E. Caporali. 2012a. "A Mechanistic Ecohydrological Model to Investigate Complex Interactions in Cold and Warm Water-Controlled Environments: 1. Theoretical Framework and Plot-Scale Analysis." *Journal of Advances in Modeling Earth Systems* 4 (2). <https://doi.org/10.1029/2011MS000086>.
- Fatichi, S., V. Y. Ivanov, and E. Caporali. 2012b. "A Mechanistic Ecohydrological Model to Investigate Complex Interactions in Cold and Warm Water-Controlled Environments: 2. Spatiotemporal Analyses." *Journal of Advances in Modeling Earth Systems* 4 (2). <https://doi.org/10.1029/2011MS000087>.
- Fatichi, S., D. Or, R. Walko, H. Vereecken, M. Young, T. Ghezzehei, T. Hengl, et al. 2020. "Soil Structure Is an Important Omission in Earth System Models." *Nature Communications* 11:522. <https://doi.org/10.1038/s41467-020-14411-z>.
- Fatichi, S., and C. Pappas. 2017. "Constrained Variability of Modeled T:ET Ratio Across Biomes." *Geophysical Research Letters* 44 (13): 6795–6803. <https://doi.org/10.1002/2017GL074041>.
- Fatichi, S., N. Peleg, T. Mastrotheodoros, C. Pappas, and G. Manoli. "An Ecohydrological Journey of 4500 Years Reveals a Stable but Threatened Precipitation–Groundwater Recharge Relation Around Jerusalem." *Science Advances* 7 (37): eabe6303. <https://doi.org/10.1126/sciadv.abe6303>.
- Fatichi, S., E. R. Vivoni, F. L. Ogden, V. Y. Ivanov, B. Mirus, D. Gochis, C. W. Downer, et al. 2016. "An Overview of Current Applications, Challenges, and Future Trends in Distributed Process-Based Models in Hydrology." *Journal of Hydrology* 537:45–60. <https://doi.org/10.1016/j.jhydrol.2016.03.026>.
- Feldman, A. F., D. J. Short Gianotti, J. Dong, R. Akbar, W. T. Crow, K. A. Mccoll, A. G. Konings, et al. 2023. "Remotely Sensed Soil Moisture Can Capture Dynamics Relevant to Plant Water Uptake." *Water Resources Research* 59 (2): e2022WR033814. <https://doi.org/10.1029/2022WR033814>.
- Feng, C., L. Yang, and L. Han. 2021. "Impacts of Climate Change on Blue and Green Water Resources in the Xiangjiang River Basin of the Yangtze River, China." *Frontiers in Earth Science* 9. <https://doi.org/10.3389/feart.2021.677191>.
- Fisher, R. A., and C. D. Koven. 2020. "Perspectives on the Future of Land Surface Models and the Challenges of Representing Complex Terrestrial Systems." *Journal of Advances in Modeling Earth Systems* 12 (4): e2018MS001453. <https://doi.org/10.1029/2018MS001453>.
- Fisher, J. B., B. Lee, A. J. Purdy, G. H. Halverson, M. B. Dohlen, K. Cawse-Nicholson, A. Wang, et al. 2020. "ECOSTRESS: NASA's Next Generation Mission to Measure Evapotranspiration from the International Space Station." *Water Resources Research* 56 (4): e2019WR026058. <https://doi.org/10.1029/2019WR026058>.
- Foster, L. A., B. W. Brock, M. E. J. Cutler, and F. Diotri. 2012. "A Physically Based Method for Estimating Supraglacial Debris Thickness from Thermal Band Remote-Sensing Data." *Journal of Glaciology* 58 (210): 677–691. <https://doi.org/10.3189/2012JoG11J194>.
- Fugazza, D., A. Senese, R. S. Azzoni, M. Maugeri, D. Maragno, and G. A. Diolaiuti. 2019. "New Evidence of Glacier Darkening in the Ortles-Cevedale Group from Landsat Observations." *Global and Planetary Change* 178:35–45. <https://doi.org/10.1016/j.gloplacha.2019.04.014>.
- Fugger, S., C. L. Fyffe, S. Fatichi, E. Miles, M. Mccarthy, T. E. Shaw, B. Ding, et al. 2022. "Understanding Monsoon Controls on the Energy and Mass Balance of Glaciers in the Central and Eastern Himalaya." *The Cryosphere* 16 (5): 1631–1652. <https://doi.org/10.5194/tc-16-1631-2022>.

- Fyffe, C. L., E. Potter, S. Fugger, A. Orr, S. Fatichi, E. Loarte, K. Medina, et al. 2021. "The Energy and Mass Balance of Peruvian Glaciers." *Journal of Geophysical Research Atmospheres* 126 (23): e2021JD034911. <https://doi.org/10.1029/2021JD034911>.
- Fyffe, C. L., A. S. Woodget, M. P. Kirkbride, P. Deline, M. J. Westoby, and B. W. Brock. 2020. "Processes at the Margins of Supraglacial Debris Cover: Quantifying Dirty Ice Ablation and Debris Redistribution." *Earth Surface Processes and Landforms* 45 (10): 2272–2290. <https://doi.org/10.1002/esp.4879>.
- Gabbi, J., M. Carenzo, F. Pellicciotti, A. Bauder, and M. Funk. 2014. "A Comparison of Empirical and Physically Based Glacier Surface Melt Models for Long-Term Simulations of Glacier Response." *Journal of Glaciology* 60 (224): 1140–1154. <https://doi.org/10.3189/2014JG14J011>.
- Gardner, A., M. Fahnestock, and T. Scambos. 2022. "MEaSures ITS\_LIVE Regional Glacier and Ice Sheet Surface Velocities, Version 1." Boulder, Colorado USA: NASA National Snow and Ice Data Center Distributed Active Archive Center. Accessed May 30, 2023. <https://doi.org/10.5067/6II6VW8LLWJ7>.
- Grant, G. E., and W. E. Dietrich. 2017. "The Frontier Beneath Our Feet." *Water Resources Research* 53 (4): 2605–2609. <https://doi.org/10.1002/2017WR020835>.
- Hall, D. K., and G. A. Riggs. 2020. "MODIS/Terra CGF Snow Cover Daily L3 Global 500m SIN Grid, Version 61 [Data Set]. Boulder, Colorado USA." NASA National Snow and Ice Data Center Distributed Active Archive Center. Accessed August 10, 2022. <https://doi.org/10.5067/MODIS/MOD10A1F.061>.
- Hall, D. K., G. A. Riggs, and V. V. Salomonson. 1995. "Development of Methods for Mapping Global Snow Cover Using Moderate Resolution Imaging Spectroradiometer Data." *Remote Sensing of Environment* 54 (2): 127–140. [https://doi.org/10.1016/0034-4257\(95\)00137-P](https://doi.org/10.1016/0034-4257(95)00137-P).
- Herreid, S., and F. Pellicciotti. 2020. "The State of Rock Debris Covering Earth's Glaciers." *Nature Geoscience* 13 (9): 621–627. <https://doi.org/10.1038/s41561-020-0615-0>.
- Hewitt, K. 2005. "The Karakoram Anomaly? Glacier Expansion and the 'Elevation Effect,' Karakoram Himalaya." *Mountain Research and Development* 25 (4): 332–340. [https://doi.org/10.1659/0276-4741\(2005\)025\[0332:TKAGEA\]2.0.CO;2](https://doi.org/10.1659/0276-4741(2005)025[0332:TKAGEA]2.0.CO;2).
- Hewitt, K. 2011. "Glacier Change, Concentration, and Elevation Effects in the Karakoram Himalaya, Upper Indus Basin." *Mountain Research and Development* 31 (3): 188–200. <https://doi.org/10.1659/MRD-JOURNAL-D-11-00020.1>.
- Hiller, R., M. J. Zeeman, and W. Eugster. 2008. "Eddy-Covariance Flux Measurements in the Complex Terrain of an Alpine Valley in Switzerland." *Boundary-Layer Meteorology* 127 (3): 449–467. <https://doi.org/10.1007/s10546-008-9267-0>.
- Hock, R. 2003. "Temperature Index Melt Modelling in Mountain Areas." *Journal of Hydrology* 282 (1): 104–115. [https://doi.org/10.1016/S0022-1694\(03\)00257-9](https://doi.org/10.1016/S0022-1694(03)00257-9).
- Huang, Q., D. Long, M. Du, Z. Han, and P. Han. 2020. "Daily Continuous River Discharge Estimation for Ungauged Basins Using a Hydrologic Model Calibrated by Satellite Altimetry: Implications for the SWOT Mission." *Water Resources Research* 56 (7): e2020WR027309. <https://doi.org/10.1029/2020WR027309>.
- Huang, Q., D. Long, M. Du, C. Zeng, G. Qiao, X. Li, A. Hou, and Y. Hong. 2018. "Discharge Estimation in High-Mountain Regions with Improved Methods Using Multisource Remote Sensing: A Case Study of the Upper Brahmaputra River." *Remote Sensing of Environment* 219:115–134. <https://doi.org/10.1016/j.rse.2018.10.008>.
- Huete, A., K. Didan, T. Miura, E. P. Rodriguez, X. Gao, and L. G. Ferreira. 2002. "Overview of the Radiometric and Biophysical Performance of the MODIS Vegetation Indices." *Remote Sensing of Environment* 83 (1–2): 195–213. [https://doi.org/10.1016/S0034-4257\(02\)00096-2](https://doi.org/10.1016/S0034-4257(02)00096-2).
- Hugonnet, R., R. McNabb, E. Berthier, B. Menounos, C. Nuth, L. Girod, D. Farinotti, et al. 2021. "Accelerated Global Glacier Mass Loss in the Early Twenty-First Century." *Nature* 592 (7856): 726–731. <https://doi.org/10.1038/s41586-021-03436-z>.
- Huss, M., and R. Hock. 2018. "Global-Scale Hydrological Response to Future Glacier Mass Loss." *Nature Climate Change* 8 (2): 135–140. <https://doi.org/10.1038/s41586-017-0049-x>.
- Immerzeel, W. W., A. F. Lutz, M. Andrade, A. Bahl, H. Biemans, T. Bolch, S. Hyde, et al. 2020. "Importance and Vulnerability of the World's Water Towers." *Nature* 577 (7790): 364–369. <https://doi.org/10.1038/s41586-019-1822-y>.
- Immerzeel, W. W., F. Pellicciotti, and M. F. P. Bierkens. 2013. "Rising River Flows Throughout the Twenty-First Century in Two Himalayan Glacierized Watersheds." *Nature Geoscience* 6 (9): 742–745. <https://doi.org/10.1038/ngeo1896>.
- Immerzeel, W. W., F. Pellicciotti, and A. B. Shrestha. 2012. "Glaciers As a Proxy to Quantify the Spatial Distribution of Precipitation in the Hunza Basin." *Mountain Research and Development* 32 (1): 30–38. <https://doi.org/10.1659/MRD-JOURNAL-D-11-00097.1>.
- Immerzeel, W. W., L. Petersen, S. Ragetti, and F. Pellicciotti. 2014. "The Importance of Observed Gradients of Air Temperature and Precipitation for Modeling Runoff from a Glacierized Watershed in the Nepalese Himalayas." *Water Resources Research* 50 (3): 2212–2226. <https://doi.org/10.1002/2013WR014506>.
- Immerzeel, W. W., L. P. H. Van Beek, and M. F. P. Bierkens. 2010. "Climate Change Will Affect the Asian Water Towers." *Science* 328 (5984): 1382–1385. <https://doi.org/10.1126/science.1183188>.
- Ivanov, V. Y., R. L. Bras, and E. R. Vivoni. 2008. "Vegetation-Hydrology Dynamics in Complex Terrain of Semiarid Areas: 1. A Mechanistic Approach to Modeling Dynamic Feedbacks." *Water Resources Research* 44:3. <https://doi.org/10.1029/2006WR005588>.
- Jacob, T., J. Wahr, W. T. Pfeffer, and S. Swenson. 2012. "Recent Contributions of Glaciers and Ice Caps to Sea Level Rise." *Nature* 482 (7386): 514–518. <https://doi.org/10.1038/nature10847>.
- Jakob, L., and N. Gourmelen. 2023. "Glacier Mass Loss Between 2010 and 2020 Dominated by Atmospheric Forcing." *Geophysical Research Letters* 50 (8): e2023GL102954. <https://doi.org/10.1029/2023GL102954>.
- Jolly, W. M., M. Dobbertin, N. E. Zimmermann, and M. Reichstein. 2005. "Divergent Vegetation Growth Responses to the 2003 Heat Wave in the Swiss Alps." *Geophysical Research Letters* 32:18. <https://doi.org/10.1029/2005GL023252>.
- Jouberton, A., T. E. Shaw, E. Miles, M. McCarthy, S. Fugger, S. Ren, A. Dehecq, W. Yang, and F. Pellicciotti. 2022. "Warming-Induced Monsoon Precipitation Phase Change Intensifies Glacier Mass Loss in the

- Southeastern Tibetan Plateau.” *Proceedings of the National Academy of Sciences* 119 (37): e2109796119. <https://doi.org/10.1073/pnas.2109796119>.
- Jung, M., S. Koirala, U. Weber, K. Ichii, F. Gans, G. Camps-Valls, D. Papale, et al. 2019. “The Fluxcom Ensemble of Global Land-Atmosphere Energy Fluxes.” *Scientific Data* 6 (1): 74. <https://doi.org/10.1038/s41597-019-0076-8>.
- Kennedy, D., S. Swenson, K. W. Oleson, D. M. Lawrence, R. Fisher, A. C. Lola Da Costa, and P. Gentine. 2019. “Implementing Plant Hydraulics in the Community Land Model, Version 5.” *Journal of Advances in Modeling Earth Systems* 11 (2): 485–513. <https://doi.org/10.1029/2018MS001500>.
- Kerr, Y. H., P. Waldteufel, P. Richaume, J. P. Wigneron, P. Ferrazzoli, A. Mahmoodi, A. A. Bitar, et al. 2012. “The SMOS Soil Moisture Retrieval Algorithm.” *IEEE Transactions on Geoscience & Remote Sensing* 50 (5): 1384–1403. <https://doi.org/10.1109/TGRS.2012.2184548>.
- Keune, J., and D. G. Miralles. 2019. “A Precipitation Recycling Network to Assess Freshwater Vulnerability: Challenging the Watershed Convention.” *Water Resources Research* 55 (11): 9947–9961. <https://doi.org/10.1029/2019WR025310>.
- Kim, S., Y. Y. Liu, F. M. Johnson, R. M. Parinussa, and A. Sharma. 2015. “A Global Comparison of Alternate AMSR2 Soil Moisture Products: Why Do They Differ?” *Remote Sensing of Environment* 161:43–62. <https://doi.org/10.1016/j.rse.2015.02.002>.
- Kneib, M., E. S. Miles, P. Buri, P. Molnar, M. McCarthy, S. Fugger, and F. Pellicciotti. 2021b. “Interannual Dynamics of Ice Cliff Populations on Debris-Covered Glaciers from Remote Sensing Observations and Stochastic Modeling.” *Journal of Geophysical Research: Earth Surface* 126 (10): e2021JF006179. <https://doi.org/10.1029/2021JF006179>.
- Kneib, M., E. S. Miles, S. Jola, P. Buri, S. Herreid, A. Bhattacharya, C. S. Watson, et al. 2021a. “Mapping Ice Cliffs on Debris-Covered Glaciers Using Multispectral Satellite Images.” *Remote Sensing of Environment* 253:112201. <https://doi.org/10.1016/j.rse.2020.112201>.
- Köhler, P., C. Frankenberg, T. S. Magney, L. Guanter, J. Joiner, and J. Landgraf. 2018. “Global Retrievals of Solar-Induced Chlorophyll Fluorescence with TROPOMI: First Results and Intersensor Comparison to OCO-2.” *Geophysical Research Letters* 45 (19): 10,456–410,463. <https://doi.org/10.1029/2018GL079031>.
- Konz, M., S. Uhlenbrook, L. Braun, A. Shrestha, and S. Demuth. 2007. “Implementation of a Process-Based Catchment Model in a Poorly Gauged, Highly Glacierized Himalayan Headwater.” *Hydrology and Earth System Sciences* 11 (4): 1323–1339. <https://doi.org/10.5194/hess-11-1323-2007>.
- Kraaijenbrink, P. D. A., M. F. P. Bierkens, A. F. Lutz, and W. W. Immerzeel. 2017. “Impact of a Global Temperature Rise of 1.5 Degrees Celsius on Asia’s Glaciers.” *Nature* 549 (7671): 257–260. <https://doi.org/10.1038/nature23878>.
- Kraaijenbrink, P., E. Stigter, T. Yao, and W. W. Immerzeel. 2021. “Climate Change Decisive for Asia’s Snow Meltwater Supply.” *Nature Climate Change* 11:1–7. <https://doi.org/10.1038/s41558-021-01074-x>.
- Krajčí, P., L. Holko, R. Perdigao, and J. Parajka. 2014. “Estimation of Regional Snowline Elevation (RSLE) from MODIS Images for Seasonally Snow Covered Mountain Basins.” *Journal of Hydrology* 519:1769–1778. <https://doi.org/10.1016/j.jhydrol.2014.08.064>.
- Lansu, E., C. Van Heerwaarden, A. Stegehuis, and A. Teuling. 2020. “Atmospheric Aridity and Apparent Soil Moisture Drought in European Forest During Heat Waves.” *Geophysical Research Letters* 47 (6): e2020GL087091. <https://doi.org/10.1029/2020GL087091>.
- Law, B. E., A. Cescatti, and D. D. Baldocchi. 2001. “Leaf Area Distribution and Radiative Transfer in Open-Canopy Forests: Implications for Mass and Energy Exchange.” *Tree Physiology* 21 (12–13): 777–787. <https://doi.org/10.1093/treephys/21.12-13.777>.
- Lin, Y. S., B. E. Medlyn, R. A. Duursma, I. C. Prentice, H. Wang, S. Baig, D. Eamus, et al. 2015. “Optimal Stomatal Behaviour Around the World.” *Nature Climate Change* 5 (5): 459–464. <https://doi.org/10.1038/nclimate2550>.
- Litt, M., J. Shea, P. Wagnon, J. Steiner, I. Koch, E. Stigter, and W. Immerzeel. 2019. “Glacier Ablation and Temperature Indexed Melt Models in the Nepalese Himalaya.” *Scientific Reports* 9 (1): 5264. <https://doi.org/10.1038/s41598-019-41657-5>.
- Loomis, B. D., A. S. Richey, A. A. Arendt, R. Appana, Y. J. C. Deweese, B. A. Forman, S. V. Kumar, T. J. Sabaka, and D. E. Shean. 2019. “Water Storage Trends in High Mountain Asia.” *Frontiers in Earth Science* 7:235. <https://doi.org/10.3389/feart.2019.00235>.
- Maes, W., B. Pagán, B. Martens, P. Gentine, L. Guanter, K. Steppe, N. Verhoest, et al. 2020. “Sun-Induced Fluorescence Closely Linked to Ecosystem Transpiration As Evidenced by Satellite Data and Radiative Transfer Models.” *Remote Sensing of Environment* 249:112030. <https://doi.org/10.1016/j.rse.2020.112030>.
- Maina, F. Z., S. V. Kumar, C. Albergel, and S. P. Mahanama. 2022. “Warming, Increase in Precipitation, and Irrigation Enhance Greening in High Mountain Asia.” *Communications Earth & Environment* 3 (1): 43. <https://doi.org/10.1038/s43247-022-00374-0>.
- Manoli, G., V. Y. Ivanov, and S. Fatichi. 2018. “Dry-Season Greening and Water Stress in Amazonia: The Role of Modeling Leaf Phenology.” *Journal of Geophysical Research: Biogeosciences* 123 (6): 1909–1926. <https://doi.org/10.1029/2017JG004282>.
- Martens, B., D. G. Miralles, H. Lievens, R. Van Der Schalie, R. A. M. De Jeu, D. Fernández-Prieto, H. E. Beck, W. A. Dorigo, and N. E. C. Verhoest. 2017. “GLEAM v3: Satellite-Based Land Evaporation and Root-Zone Soil Moisture.” *Geoscientific Model Development* 10 (5): 1903–1925. <https://doi.org/10.5194/gmd-10-1903-2017>.
- Marzeion, B., R. Hock, B. Anderson, A. Bliss, N. Champollion, K. Fujita, M. Huss, et al. 2020. “Partitioning the Uncertainty of Ensemble Projections of Global Glacier Mass Change.” *Earth’s Future* 8 (7): e2019EF001470. <https://doi.org/10.1029/2019EF001470>.
- Mastrotheodoros, T., C. Pappas, P. Molnar, P. Burlando, P. Hadjidoukas, and S. Fatichi. 2019. “Ecohydrological Dynamics in the Alps: Insights from a Modelling Analysis of the Spatial Variability.” *Ecohydrology* 12 (1): e2054. <https://doi.org/10.1002/eco.2054>.
- Mastrotheodoros, T., C. Pappas, P. Molnar, P. Burlando, G. Manoli, J. Parajka, R. Rigon, et al. 2020. “More Green and Less Blue Water in the Alps During Warmer Summers.” *Nature Climate Change* 10 (2): 155–161. <https://doi.org/10.1038/s41558-019-0676-5>.
- Maxwell, R. M., and S. J. Kollet. 2008. “Quantifying the Effects of Three-Dimensional Subsurface Heterogeneity on Hortonian Runoff Processes Using a Coupled Numerical, Stochastic Approach.” *Advances in Water*

- Resources* 31 (5): 807–817. <https://doi.org/10.1016/j.advwatres.2008.01.020>.
- McCarthy, M. J. 2018. “Quantifying Supraglacial Debris Thickness at Local to Regional Scales.” Doctoral diss., University of Cambridge.
- McCarthy, M., E. Miles, M. Kneib, P. Buri, S. Fugger, and F. Pellicciotti. 2022. “Supraglacial Debris Thickness and Supply Rate in High-Mountain Asia.” *Communications Earth & Environment* 3 (1): 269. <https://doi.org/10.1038/s43247-022-00588-2>.
- Miehe, G., S. Miehe, J. Vogel, and D. La. 2007. “Highest Treeline in the Northern Hemisphere Found in Southern Tibet.” *Mountain Research and Development* 27 (2): 169–173. <https://doi.org/10.1659/mrd.0792>.
- Mihalcea, C., C. Mayer, G. Diolaiuti, C. D’Agata, C. Smiraglia, A. Lambrecht, E. Vuillermoz, and G. Tartari. 2008. “Spatial Distribution of Debris Thickness and Melting From Remote-Sensing and Meteorological Data, at Debris-Covered Baltoro Glacier, Karakoram, Pakistan.” *Annals of Glaciology* 48:49–57. <https://doi.org/10.3189/172756408784700680>.
- Miles, E., M. McCarthy, A. Dehecq, M. Kneib, S. Fugger, and F. Pellicciotti. 2021. “Health and Sustainability of Glaciers in High Mountain Asia.” *Nature Communications* 12 (1): 2868. <https://doi.org/10.1038/s41467-021-23073-4>.
- Miles, E. S., J. F. Steiner, P. Buri, W. W. Immerzeel, and F. Pellicciotti. 2022. “Controls on the Relative Melt Rates of Debris-Covered Glacier Surfaces.” *Environmental Research Letters* 17 (6): 064004. <https://doi.org/10.1088/1748-9326/ac6966>.
- Miles, E. S., J. Steiner, I. Willis, P. Buri, W. W. Immerzeel, A. Chesnokova, and F. Pellicciotti. 2017. “Pond Dynamics and Supraglacial-Englacial Connectivity on Debris-Covered Lirung Glacier, Nepal.” *Frontiers in Earth Science* 5. <https://doi.org/10.3389/feart.2017.00069>.
- Miles, E., I. Willis, P. Buri, J. Steiner, N. Arnold, and F. Pellicciotti. 2018. “Surface Pond Energy Absorption Across Four Himalayan Glaciers Accounts for 1/8 of Total Catchment Ice Loss.” *Geophysical Research Letters* 45 (19): 10464–10473. <https://doi.org/10.1029/2018GL079678>.
- Millan, R., J. Mouginot, A. Rabatel, and M. Morlighem. 2023. “Author Correction: Ice Velocity and Thickness of the world’s Glaciers.” *Nature Geoscience* 16 (2): 188–188. <https://doi.org/10.1038/s41561-022-01106-x>.
- Milner, A. M., K. Khamis, T. J. Battin, J. E. Brittain, N. E. Barrand, L. Füreder, S. Cauvy-Fraunié, et al. 2017. “Glacier Shrinkage Driving Global Changes in Downstream Systems.” *Proceedings of the National Academy of Sciences* 114 (37): 9770–9778. <https://doi.org/10.1073/pnas.1619807114>.
- Mimeau, L., M. Esteves, I. Zin, H. W. Jacobi, F. Brun, P. Wagnon, D. Koirala, and Y. Arnaud. 2019. “Quantification of Different Flow Components in a High-Altitude Glacierized Catchment (Dudh Koshi, Himalaya): Some Cryospheric-Related Issues.” *Hydrology Earth System Sciences* 23 (9): 3969–3996. <https://doi.org/10.5194/hess-23-3969-2019>.
- Misra, A., A. Kumar, R. Bhambri, U. Haritashya, A. Verma, D. Dobhal, A. Gupta, G. Gupta, and R. Upadhyay. 2020. “Topographic and Climatic Influence on Seasonal Snow Cover: Implications for the Hydrology of Ungauged Himalayan Basins, India.” *Journal of Hydrology* 124716. <https://doi.org/10.1016/j.jhydrol.2020.124716>.
- Munier, S., D. Carrer, C. Planque, F. Camacho, C. Albergel, and J. C. Calvet. 2018. “Satellite Leaf Area Index: Global Scale Analysis of the Tendencies per Vegetation Type Over the Last 17 Years.” *Remote Sensing* 10 (3): 424. <https://doi.org/10.3390/rs10030424>.
- Mu, Q., M. Zhao, and S. W. Running. 2011. “Improvements to a MODIS Global Terrestrial Evapotranspiration Algorithm.” *Remote Sensing of Environment* 115 (8): 1781–1800. <https://doi.org/10.1016/j.rse.2011.02.019>.
- Myneni, R., and Y. Knyazkhin. 2018. *VIIRS/NPP Leaf Area Index/FPAR 8-Day LA Global 500m SIN Grid V001*. NASA EOSDIS Land Processes DAAC.
- Naegeli, K., A. Damm, M. Huss, H. Wulf, M. Schaepman, and M. Hoelzle. 2017. “Cross-Comparison of Albedo Products for Glacier Surfaces Derived from Airborne and Satellite (Sentinel-2 and Landsat 8) Optical Data.” *Remote Sensing* 9 (2): 110. <https://doi.org/10.3390/rs9020110>.
- Naegeli, K., M. Huss, and M. Hoelzle. 2019. “Change Detection of Bare-Ice Albedo in the Swiss Alps.” *The Cryosphere* 13 (1): 397–412. <https://doi.org/10.5194/tc-13-397-2019>.
- NASA JPL 2014. “ASTER Global Emissivity Dataset, 100-meter, HDF5.” NASA EOSDIS Land Processes Distributed Active Archive Center. Accessed November 9, 2023. [https://doi.org/10.5067/Community/ASTER\\_GED/AG100.003](https://doi.org/10.5067/Community/ASTER_GED/AG100.003).
- Nie, Y., H. D. Pritchard, Q. Liu, T. Hennig, W. Wang, X. Wang, S. Liu, et al. 2021. “Glacial Change and Hydrological Implications in the Himalaya and Karakoram.” *Nature Reviews Earth and Environment* 2: 91–106. <https://doi.org/10.1038/s43017-020-00124-w>.
- Orth, R., and G. Destouni. 2018. “Drought Reduces Blue-Water Fluxes More Strongly Than Green-Water Fluxes in Europe.” *Nature Communications* 9 (1): 3602. <https://doi.org/10.1038/s41467-018-06013-7>.
- Östrem, G. 1959. “Ice Melting Under a Thin Layer of Moraine, and the Existence of Ice Cores in Moraine Ridges.” *Geografiska Annaler* 41 (4): 228–230. <https://doi.org/10.1080/20014422.1959.11907953>.
- Paschalis, A., S. Fatichi, C. Pappas, and D. Or. 2018. “Covariation of Vegetation and Climate Constrains Present and Future T/ET Variability.” *Environmental Research Letters* 13 (10): 104012. <https://doi.org/10.1088/1748-9326/aae267>.
- Pellicciotti, F., C. Buergi, W. W. Immerzeel, M. Konz, and A. B. Shrestha. 2012. “Challenges and Uncertainties in Hydrological Modeling of Remote Hindu Kush–Karakoram–Himalayan (HKH) Basins: Suggestions for Calibration Strategies.” *Mountain Research and Development* 32 (1): 39–50. <https://doi.org/10.1659/MRD-JOURNAL-D-11-00092.1>.
- Peng, J., C. Albergel, A. Balenzano, L. Brocca, O. Cartus, M. H. Cosh, W. T. Crow, et al. 2021. “A Roadmap for High-Resolution Satellite Soil Moisture Applications – Confronting Product Characteristics with User Requirements.” *Remote Sensing of Environment* 252:112162. <https://doi.org/10.1016/j.rse.2020.112162>.
- Pickering, M., A. Cescatti, and G. Duveiller. 2022. “Sun-Induced Fluorescence As a Proxy for Primary Productivity Across Vegetation Types and Climates.” *Biogeosciences* 19 (20): 4833–4864. <https://doi.org/10.5194/bg-19-4833-2022>.
- Potocki, M., P. A. Mayewski, T. Matthews, L. B. Perry, M. Schwikowski, A. M. Tait, E. Korotkikh, et al. 2022. “Mt. Everest’s Highest Glacier Is a Sentinel for Accelerating Ice Loss.” *npj Climate and Atmospheric Science* 5 (1): 7. <https://doi.org/10.1038/s41612-022-00230-0>.



- Pritchard, H. D. 2019. "Asia's Shrinking Glaciers Protect Large Populations from Drought Stress." *Nature* 569 (7758): 649–654. <https://doi.org/10.1038/s41586-019-1240-1>.
- Pritchard, H. D. 2021. "Global Data Gaps in Our Knowledge of the Terrestrial Cryosphere." *Frontiers in Climate* 3:689823. <https://doi.org/10.3389/fclim.2021.689823>.
- Racoviteanu, A. E., L. Nicholson, and N. F. Glasser. 2021. "Surface Composition of Debris-Covered Glaciers Across the Himalaya Using Linear Spectral Unmixing of Landsat 8 OLI Imagery." *The Cryosphere* 15 (9): 4557–4588. <https://doi.org/10.5194/tc-15-4557-2021>.
- Ragetli, S., W. W. Immerzeel, and F. Pellicciotti. 2016. "Contrasting Climate Change Impact on River Flows from High-Altitude Catchments in the Himalayan and Andes Mountains." *Proceedings of the National Academy of Sciences* 113 (33): 9222–9227. <https://doi.org/10.1073/pnas.1606526113>.
- Ragetli, S., F. Pellicciotti, R. Bordoy, and W. W. Immerzeel. 2013. "Sources of Uncertainty in Modeling the Glaciohydrological Response of a Karakoram Watershed to Climate Change." *Water Resources Research* 49 (9): 6048–6066. <https://doi.org/10.1002/wrcr.20450>.
- Ragetli, S., F. Pellicciotti, W. W. Immerzeel, E. S. Miles, L. Petersen, M. Heynen, J. M. Shea, et al. 2015. "Unraveling the Hydrology of a Himalayan Catchment Through Integration of High Resolution in situ Data and Remote Sensing with an Advanced Simulation Model." *Advances in Water Resources* 78:94–111. <https://doi.org/10.1016/j.advwatres.2015.01.013>.
- Ren, S., E. S. Miles, L. Jia, M. Menenti, M. Kneib, P. Buri, M. J. McCarthy, T. E. Shaw, W. Yang, and F. Pellicciotti. 2021. "Anisotropy Parameterization Development and Evaluation for Glacier Surface Albedo Retrieval from Satellite Observations." *Remote Sensing* 13 (9): 1714. <https://doi.org/10.3390/rs13091714>.
- Rittger, K., T. H. Painter, and J. Dozier. 2013. "Assessment of Methods for Mapping Snow Cover from MODIS." *Advances in Water Resources* 51:367–380. <https://doi.org/10.1016/j.advwatres.2012.03.002>.
- Rockström, J., M. Falkenmark, L. Karlberg, H. Hoff, S. Rost, and D. Gerten. 2009. "Future Water Availability for Global Food Production: The Potential of Green Water for Increasing Resilience to Global Change." *Water Resources Research* 45:7. <https://doi.org/10.1029/2007WR006767>.
- Rockström, J., M. Mazzucato, L. Andersen, S. Fahrländer, and D. Gerten. 2023. "Why We Need a New Economics of Water As a Common Good." *Nature* 615. <https://doi.org/10.1038/d41586-023-00800-z>.
- Rounce, D. R., R. Hock, F. Maussion, R. Hugonnet, W. Kochtitzky, M. Huss, E. Berthier, et al. 2023. "Global Glacier Change in the 21st Century: Every Increase in Temperature Matters." *Science* 379 (6627): 78–83. <https://doi.org/10.1126/science.abo1324>.
- Rounce, D. R., R. Hock, R. W. McNabb, R. Millan, C. Sommer, M. H. Braun, P. Malz, et al. 2021. "Distributed Global Debris Thickness Estimates Reveal Debris Significantly Impacts Glacier Mass Balance." *Geophysical Research Letters* 48 (8): e2020GL091311. <https://doi.org/10.1029/2020GL091311>.
- Rounce, D. R., O. King, M. McCarthy, D. E. Shean, and F. Salerno. 2018. "Quantifying Debris Thickness of Debris-Covered Glaciers in the Everest Region of Nepal Through Inversion of a Subdebris Melt Model." *Journal of Geophysical Research: Earth Surface* 123 (5): 1094–1115. <https://doi.org/10.1029/2017JF004395>.
- Rounce, D. R., and D. C. McKinney. 2014. "Debris Thickness of Glaciers in the Everest Area (Nepal Himalaya) Derived from Satellite Imagery Using a Nonlinear Energy Balance Model." *The Cryosphere* 8 (4): 1317–1329. <https://doi.org/10.5194/tc-8-1317-2014>.
- Running, S., Q. Mu, and M. Zhao. 2015. "MOD17A2H MODIS/Terra Gross Primary Productivity 8-Day L4 Global 500m SIN Grid V006." NASA EOSDIS Land Processes DAAC. NASA EOSDIS Land Processes Distributed Active Archive Center. Accessed January 19, 2024. <https://doi.org/10.5067/MODIS/MOD17A2H.006>.
- Scanlon, B. R., Z. Zhang, H. Save, A. Y. Sun, H. Müller Schmied, L. P. H. Van Beek, D. N. Wiese, et al. 2018. "Global models underestimate large decadal declining and rising water storage trends relative to grace satellite data." *Proceedings of the National Academy of Sciences* 115 (6): E1080–E1089. <https://doi.org/10.1073/pnas.1704665115>.
- Schauwecker, S., M. Rohrer, C. Huggel, A. Kulkarni, A. Ramanathan, N. Salzmann, M. Stoffel, and B. Brock. 2015. "Remotely Sensed Debris Thickness Mapping of Bara Shigri Glacier, Indian Himalaya." *Journal of Glaciology* 61 (228): 675–688. <https://doi.org/10.3189/2015JG14J102>.
- Scherler, D., H. Wulf, and N. Gorelick. 2018. "Global Assessment of Supraglacial Debris-Cover Extents." *Geophysical Research Letters* 45 (21): 11798–11805. <https://doi.org/10.1029/2018GL080158>.
- Shaw, T. E., A. Caro, P. Mendoza, Á. Ayala, F. Pellicciotti, S. Gascoin, and J. McPhee. 2020a. "The Utility of Optical Satellite Winter Snow Depths for Initializing a Glacio-Hydrological Model of a High-Elevation, Andean Catchment." *Water Resources Research* 56 (8): e2020WR027188. <https://doi.org/10.1029/2020WR027188>.
- Shaw, T. E., E. S. Miles, D. Chen, A. Jouberton, M. Kneib, S. Fugger, T. Ou, et al. 2022. "Multi-Decadal Monsoon Characteristics and Glacier Response in High Mountain Asia." *Environmental Research Letters* 17 (10): 104001. <https://doi.org/10.1088/1748-9326/ac9008>.
- Shaw, T. E., G. Ulloa, D. Fariás-Barahona, R. Fernandez, J. M. Lattus, and J. McPhee. 2020b. "Glacier Albedo Reduction and Drought Effects in the Extratropical Andes, 1986 – 2020." *Journal of Glaciology* 67 (261): 158–169. <https://doi.org/10.1017/jog.2020.102>.
- Sheffield, J., E. F. Wood, and M. L. Roderick. 2012. "Little Change in Global Drought Over the Past 60 Years." *Nature* 491 (7424): 435–438. <https://doi.org/10.1038/nature11575>.
- Shen, C., L. Jia, and S. Ren. 2022. "Inter- and Intra-Annual Glacier Elevation Change in High Mountain Asia Region Based on ICESat-1&2 Data Using Elevation-Aspect Bin Analysis Method." *Remote Sensing* 14 (7): 1630. <https://doi.org/10.3390/rs14071630>.
- Sherpa, T. C., T. Matthews, L. B. Perry, A. Thapa, P. K. Singh, A. Khadka, I. Koch, et al. 2023. "Insights from the First Winter Weather Observations Near Mount Everest's Summit." *Weather* 78 (12): 344–348. <https://doi.org/10.1002/wea.4374>.
- Small, C. 2021. "Grand Challenges in Remote Sensing Image Analysis and Classification." *Frontiers in Remote Sensing* 1:605220. <https://doi.org/10.3389/frsen.2020.605220>.
- Sood, A., S. A. Prathapar, and V. Smakhtin. 2014. "Green and Blue Water." In *Key Concepts in Water Resource Management: A Review and Critical Evaluation*, edited by A. Sood, 91–102. London: Routledge.

- Sorg, A., M. Huss, M. Rohrer, and M. Stoffel. 2014. "The Days of Plenty Might Soon Be Over in Glacierized Central Asian Catchments." *Environmental Research Letters* 9 (10): 104018. <https://doi.org/10.1088/1748-9326/9/10/104018>.
- Sibal, M. A.-O., J. A.-O. X. Bradley, A. Edwards, S. A.-O. Hotaling, K. Zawierucha, J. Rosvold, S. Lutz, et al. 2020. "Glacial Ecosystems Are Essential to Understanding Biodiversity Responses to Glacier Retreat." *Nature Ecology & Evolution* 4 (5): 686–687. <https://doi.org/10.1038/s41559-020-1163-0>.
- Stigter, E. E., M. Litt, J. F. Steiner, P. N. J. Bonekamp, J. M. Shea, M. F. P. Bierkens, and W. W. Immerzeel. 2018. "The Importance of Snow Sublimation on a Himalayan Glacier." *Frontiers in Earth Science* 6:108. <https://doi.org/10.3389/feart.2018.00108>.
- Stocker, B. D., S. J. Tumber-Dávila, A. G. Konings, M. C. Anderson, C. Hain, and R. B. Jackson. 2023. "Global Patterns of Water Storage in the Rooting Zones of Vegetation." *Nature Geoscience* 16 (3): 250–256. <https://doi.org/10.1038/s41561-023-01125-2>.
- Sun, Q., C. Miao, Q. Duan, H. Ashouri, S. Sorooshian, and K.-L. Hsu. 2018. "A Review of Global Precipitation Data Sets: Data Sources, Estimation, and Intercomparisons." *Reviews of Geophysics* 56 (1): 79–107. <https://doi.org/10.1002/2017RG000574>.
- Teuling, A. J. 2018. "A Hot Future for European Droughts." *Nature Climate Change* 8 (5): 364–365. <https://doi.org/10.1038/s41558-018-0154-5>.
- Teuling, A. J., S. I. Seneviratne, R. Stöckli, M. Reichstein, E. Moors, P. Ciais, S. Luysaert, et al. 2010. "Contrasting Response of European Forest and Grassland Energy Exchange to Heatwaves." *Nature Geoscience* 3 (10): 722–727. <https://doi.org/10.1038/ngeo950>.
- Van Tricht, L., P. Huybrechts, J. Van Breedam, A. Vanhulle, K. Van Oost, and H. Zekollari. 2021. "Estimating Surface Mass Balance Patterns from Unoccupied Aerial Vehicle Measurements in the Ablation Area of the Morteratsch-Pers Glacier Complex (Switzerland)." *The Cryosphere* 15 (9): 4445–4464. <https://doi.org/10.5194/tc-15-4445-2021>.
- Vicente-Serrano, S. M., J.-I. Lopez-Moreno, S. Beguería, J. Lorenzo-Lacruz, A. Sanchez-Lorenzo, J. M. García-Ruiz, C. Azorin-Molina, et al. 2014. "Evidence of Increasing Drought Severity Caused by Temperature Rise in Southern Europe." *Environmental Research Letters* 9 (4): 044001. <https://doi.org/10.1088/1748-9326/9/4/044001>.
- Viviroli, D., H. H. Dürr, B. Messerli, M. Meybeck, and R. Weingartner. 2007. "Mountains of the World, Water Towers for Humanity: Typology, Mapping, and Global Significance." *Water Resources Research* 43:7. <https://doi.org/10.1029/2006WR005653>.
- Wagner, W., S. Hahn, R. Kidd, T. Melzer, Z. Bartalis, S. Hasenauer, J. Figa-Saldaña, et al. 2013. "The ASCAT Soil Moisture Product: A Review of Its Specifications, Validation Results, and Emerging Applications." *Meteorologische Zeitschrift* 22 (1): 5–33. <https://doi.org/10.1127/0941-2948/2013/0399>.
- Wagnon, P., C. Vincent, Y. Arnaud, E. Berthier, E. Vuillemoz, S. Gruber, M. Ménégoz, et al. 2013. "Seasonal and Annual Mass Balances of Mera and Pokalde Glaciers (Nepal Himalaya) Since 2007." *The Cryosphere* 7 (6): 1769–1786. <https://doi.org/10.5194/tc-7-1769-2013>.
- Wang, Q., S. Yi, and W. Sun. 2021. "Continuous Estimates of Glacier Mass Balance in High Mountain Asia Based on ICESat-1,2 and GRACE/GRACE Follow-On Data." *Geophysical Research Letters* 48 (2): e2020GL090954. <https://doi.org/10.1029/2020GL090954>.
- Wan, Z., S. Hook, and G. Hulley. 2021. "MODIS/Terra Land Surface Temperature/Emissivity Daily L3 Global 1km SIN Grid V061." NASA EOSDIS Land Processes Distributed Active Archive Center. Accessed November 9, 2023. <https://doi.org/10.5067/MODIS/MOD11A1.061>.
- Watson, C. S., O. King, E. S. Miles, and D. J. Quincey. 2018. "Optimising NDWI Supraglacial Pond Classification on Himalayan Debris-Covered Glaciers." *Remote Sensing of Environment* 217:414–425. <https://doi.org/10.1016/j.rse.2018.08.020>.
- Winiger, M., M. Gumpert, and H. Yamout. 2005. "Karakorum–Hindukush–Western Himalaya: Assessing High-Altitude Water Resources." *Hydrological Processes* 19 (12): 2329–2338. <https://doi.org/10.1002/hyp.5887>.
- Wood, E. F., J. K. Roundy, T. J. Troy, L. P. H. Van Beek, M. F. P. Bierkens, E. Blyth, A. De Roo, et al. 2011. "Hyperresolution Global Land Surface Modeling: Meeting a Grand Challenge for Monitoring Earth's Terrestrial Water." *Water Resources Research* 47 (5). <https://doi.org/10.1029/2010WR010090>.
- Wu, S., T. Zhao, J. Pan, H. Xue, L. Zhao, and J. Shi. 2022. "Improvement in Modeling Soil Dielectric Properties During Freeze-Thaw Transitions." *IEEE Geoscience & Remote Sensing Letters* 19:1–5. <https://doi.org/10.1109/LGRS.2022.3154291>.
- Yang, Y., M. L. Roderick, H. Guo, D. G. Miralles, L. Zhang, S. Fatichi, X. Luo, et al. 2023. "Evapotranspiration on a Greening Earth." *Nature Reviews Earth and Environment* 4 (9): 626–641. <https://doi.org/10.1038/s43017-023-00464-3>.
- Yao, T., T. Bolch, D. Chen, J. Gao, W. Immerzeel, S. Piao, F. Su, et al. 2022. "The Imbalance of the Asian Water Tower." *Nature Reviews Earth and Environment* 3 (10): 618–632. <https://doi.org/10.1038/s43017-022-00299-4>.
- Yuan, L., Y. Ma, X. Chen, Y. Wang, and Z. Li. 2021. "An Enhanced MOD16 Evapotranspiration Model for the Tibetan Plateau During the Unfrozen Season." *Journal of Geophysical Research: Atmospheres* 126 (7): e2020JD032787. <https://doi.org/10.1029/2020JD032787>.
- Zeng, Y., D. Hao, A. Huete, B. Dechant, J. Berry, J. M. Chen, J. Joiner, et al. 2022. "Optical Vegetation Indices for Monitoring Terrestrial Ecosystems Globally." *Nature Reviews Earth and Environment* 3 (7): 477–493. <https://doi.org/10.1038/s43017-022-00298-5>.
- Zhang, J., L. Jia, M. Menenti, J. Zhou, and S. Ren. 2021. "Glacier Area and Snow Cover Changes in the Range System Surrounding Tarim from 2000 to 2020 Using Google Earth Engine." *Remote Sensing* 13 (24): 5117. <https://doi.org/10.3390/rs13245117>.
- Zhang, G., S. Kang, L. Cuo, and B. Qu. 2016. "Modeling Hydrological Process in a Glacier Basin on the Central Tibetan Plateau with a Distributed Hydrology Soil Vegetation Model." *Journal of Geophysical Research: Atmospheres* 121 (16): 9521–9539. <https://doi.org/10.1002/2016JD025434>.
- Zhang, Y., D. Kong, R. Gan, F. H. S. Chiew, T. R. Mcvicar, Q. Zhang, and Y. Yang. 2019. "Coupled Estimation of 500 m and 8-Day Resolution Global Evapotranspiration and Gross Primary Production in 2002–2017." *Remote Sensing of Environment* 222:165–182. <https://doi.org/10.1016/j.rse.2018.12.031>.
- Zhao, W. L., P. Gentine, M. Reichstein, Y. Zhang, S. Zhou, Y. Wen, C. Lin, X. Li, and G. Y. Qiu. 2019. "Physics-

- Constrained Machine Learning of Evapotranspiration.” *Geophysical Research Letters* 46 (24): 14496–14507. <https://doi.org/10.1029/2019GL085291>.
- Zhao, W., and A. Li. 2015. “A Review on Land Surface Processes Modelling Over Complex Terrain.” *Advances in Meteorology* 2015:607181. <https://doi.org/10.1155/2015/607181>.
- Zhao, T., J. Shi, D. Entekhabi, T. J. Jackson, L. Hu, Z. Peng, P. Yao, S. Li, and C. S. Kang. 2021. “Retrievals of Soil Moisture and Vegetation Optical Depth Using a Multi-Channel Collaborative Algorithm.” *Remote Sensing of Environment* 257:112321. <https://doi.org/10.1016/j.rse.2021.112321>.
- Zheng, C., L. Jia, and G. Hu. 2022. “Global Land Surface Evapotranspiration Monitoring by ETMonitor Model Driven by Multi-Source Satellite Earth Observations.” *Journal of Hydrology* 613:128444. <https://doi.org/10.1016/j.jhydrol.2022.128444>.
- Zhu, Z., S. Piao, R. Myneni, M. Huang, Z. Zeng, J. G. Canadell, P. Ciais, et al. 2016. “Greening of the Earth and Its Drivers.” *Nature Climate Change* 6: 791–795. <https://doi.org/10.1038/nclimate3004>.